Spring 2019

Synthesis of a stimulus responsive phosphine ligand and metal binding studies

Gabriel Bourne
Western Washington University, gbourne123@gmail.com

Synthesis of a stimulus responsive phosphine ligand and metal binding studies

By

Gabriel Bourne

Accepted in Partial Completion
of the Requirements for the Degree
Master of Science

ADVISORY COMMITTEE

Dr. Margaret Scheuermann, Chair

Dr. James Vyvyan

Dr. John Gilbertson

GRADUATE SCHOOL

Kathleen Kitto, Acting Dean

Master's Thesis

In presenting this thesis in partial fulfillment of the requirements for a master's degree at Western Washington University, I grant to Western Washington University the non-exclusive royalty-free right to archive, reproduce, distribute, and display the thesis in any and all forms, including electronic format, via any digital library mechanisms maintained by WWU.

I represent and warrant this is my original work, and does not infringe or violate any rights of others. I warrant that I have obtained written permissions from the owner of any third party copyrighted material included in these files.

I acknowledge that I retain ownership rights to the copyright of this work, including but not limited to the right to use all or part of this work in future works, such as articles or books.

Library users are granted permission for individual, research and non-commercial reproduction of this work for educational purposes only. Any further digital posting of this document requires specific permission from the author.

Any copying or publication of this thesis for commercial purposes, or for financial gain, is not allowed without my written permission.

Gabriel Bourne

May 26th 2019

Synthesis of a stimulus responsive phosphine ligand and metal binding studies

A Thesis
Presented to
The Faculty of
Western Washington University

In Partial Fulfillment
of the Requirements for the Degree
Master of Science

by
Gabriel Bourne
May 2019

Abstract

Cations have been shown to modify a variety of properties of transition metals, including bite angle, isomerization, substrate control, and catalytic activation. Herein describes the synthesis of a novel stimulus responsive phosphine ligand. Ligand binding studies by NMR salt titration show a preference in the order of $Na^+ > Li^+ > K^+$. Platinum dimethyl and dichloride complexes with the phosphine ligand were also synthesized. Isomerization of the platinum chloride complex between *cis* and *trans* is reported.

Acknowledgements

I would like to thank Dr. Margaret Scheuermann for being an amazing PI by giving me direction and guidance in helping me grow as a scientist. I would also like to thank my other committee members Dr. Vyvyan and Dr. Gilbertson for their help and support in writing this thesis.

I would also like to thank all of my fellow scientists in the Scheuermann group who have contributed to this project and created a positive lab experience.

In addition, I would like to thank all the faculty and staff at WWU who have helped me at Western. I would also like to thank WWU and NSF (award # MRI 1532269) for funding this project.

Table of Contents

List of Figures

List of Tables

Chapter 1:

Introduction

Since their discovery by Pedersen in 1967, crown ethers and polyethylene glycol chains have been shown to be useful for binding alkali metal cations.[1] In the 1980's, metallacrown ethers (crown ethers formed by chelating two ends of polyether ligand to a transition metal) were synthesized. Metallacrown ethers also selectively bind cations. This gives metallacrown ether complexes the ability to have cations influence the transition metal and its reactivity in unique ways. The general structures of crown ethers, polyethylene glycol chains, and metallacrown ethers are shown in Figure 1.1. Metallacrown ethers have been shown to have many applications in the field of asymmetric catalysis because of their tunability with the removal or addition of a cation.[2-8] This introduction will discuss how crown ethers, polyethylene glycol chains, and metallacrown ethers can be influenced by cations for the purposes of catalytic control, substrate activation, geometric control, and isomerization.

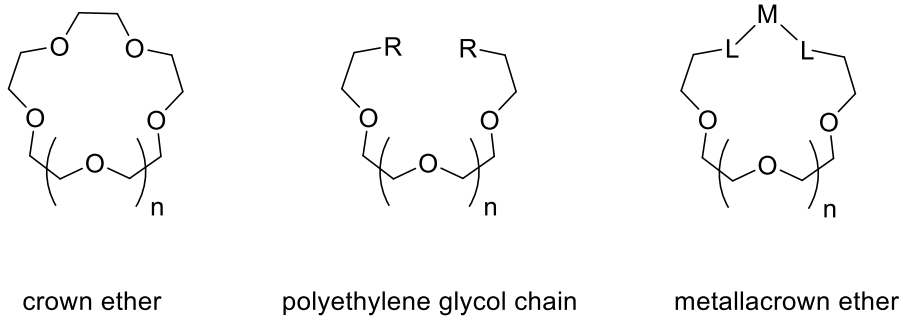

Figure 1.1. General structure of crown ethers, polyethylene glycol chains, and metallacrown ethers.

Cations and catalyst control

Catalysts are useful in a wide variety of fields for their ability to promote specific chemical transformations. In homogenous catalysis, ligands attached to a transition metal can

control the properties of the catalysis. Metallacrown ethers give catalysis an additional regulation site that can be controlled with the addition and removal of cations.

Fan and coworkers successfully synthesized a rhodium catalyst with a bidentate polyether ligand (Figure 1.2).[6] They found the enantiomeric excess varied depending on which salt was added (Figure 1.2). Without salt additive, they reported an ee of 84%. This is a lower ee% than when they added NaBArF (91%) or KBArF (93%) (BArF = $[\{3,5\text{-}(CF_3)_2C_6H_3\}_4B]^-$). They proposed the binding of the potassium or sodium ion is causing the change in selectivity. When they added 18-crown-6 to the reaction, which binds to the K^+ ion more tightly than their rhodium metallacrown ether, they saw the same reactivity as when they did not add the salt at all. In addition, they saw rate enhancement in the presence of salt. They observed full reaction conversion as monitored by ^1H NMR at approximately 25 minutes with KBArF, versus 50 minutes without the salt added.

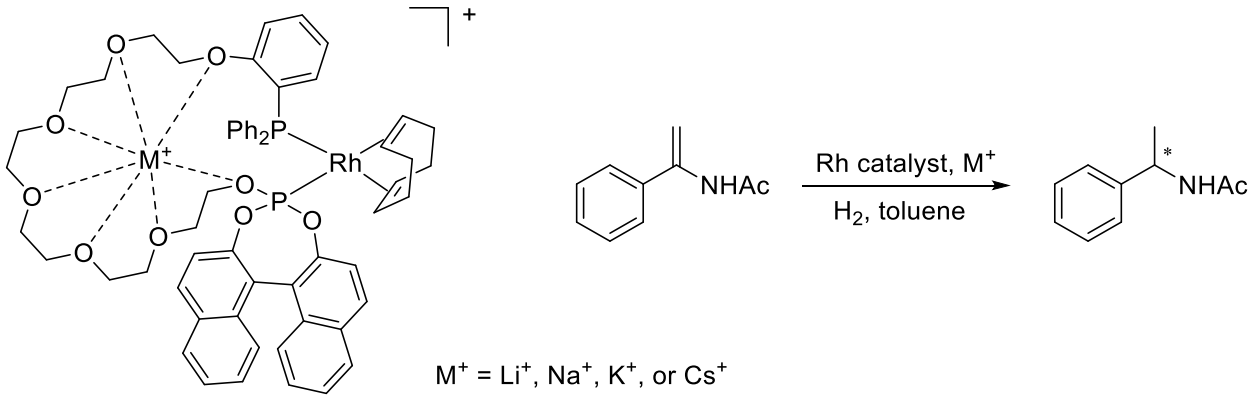

Figure 1.2. Structure of Rh catalyst (left) synthesized by Fan and coworkers. Asymmetric hydrogenation reaction of N-(1-phenylvinyl)acetamide using Rh catalyst (right).

A palladium-based catalyst reported by Vidal-Ferran and coworkers saw an increase of up to 16% ee in their allylic substitution with the use of additives such as RbOAc or $M(OTf)_x$ (M = Mg^{2+}, La^{3+}, or Ho^{3+}) (Figure 1.3).

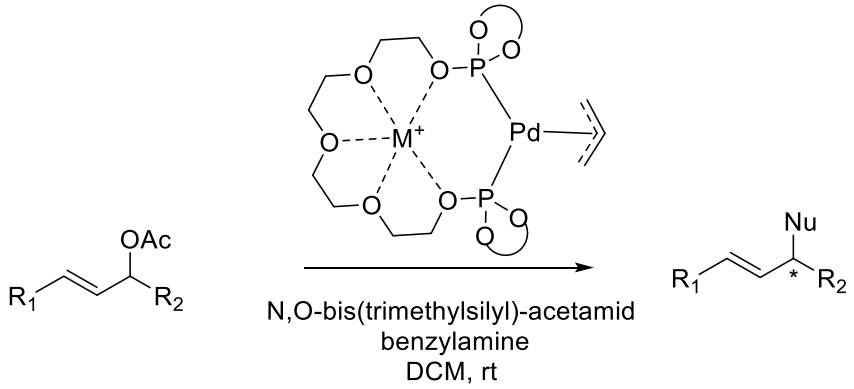

Figure 1.3 Palladium metallacrown ether catalyst used for allylic substitution (M = Mg^{2+}, La^{3+}, or Ho^{3+}).[8]

Do and Cai synthesized a nickel polyethylene glycol catalyst able to yield polyethylene with varying molecular weight and branching depending on the cation and ligand structure (Figure 1.4).[3] They also reported turnover frequencies between 1,000 and 439,000 g/((mol of Ni) hr) depending on the metal and exact ligand used. They generally saw more selective reactivity and more branching with NaBArF when compared to KBArF, which they believe has to do with the size of the glycol chain they used. They found LiBArF to inhibit polymerization, which was believed to be caused by its greater Lewis acidity inducing catalytically inactive extended structures.

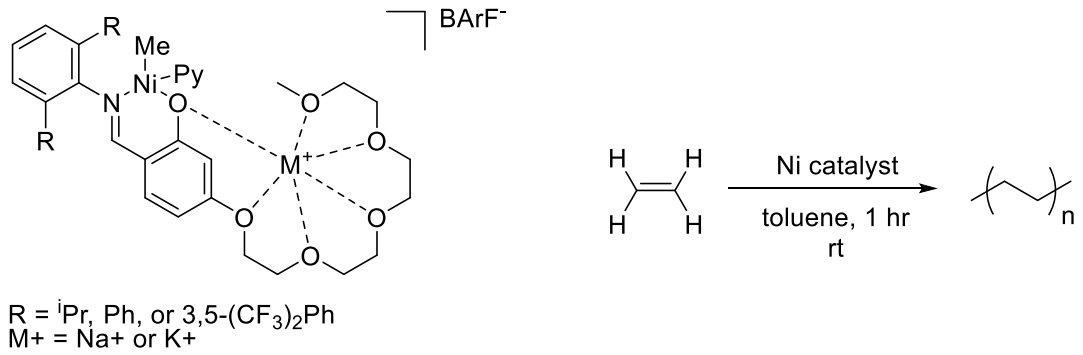

Figure 1.4. Structures of nickel catalysts synthesized by Do and Cai (left) and polyethylene polymerization reaction (right).

Fang and coworkers synthesized rhodium and iridium catalysts able to hydrogenate a variety of substrates including substituted quinolones and α-dehydroamino acid esters (Figure 1.5).[5] They found that Li^+, Na^+, and K^+ all increased the ee of their catalyst, but adding Na^+ cationic salts gave the highest ee. In addition, they observed better selectivity when using BArF as the counter anion when compared to PF_6 and BF_4, showing that the more weakly coordinating bulky anion performed better asymmetric catalysis. For example, using NaBArF achieved a >99% conversion and an ee of 93% in the hydrogenation of methyl-(*Z*)-2-acetamidocinnamate, while $NaPF_6$ only resulted in 96% conversion and an ee of 83%.

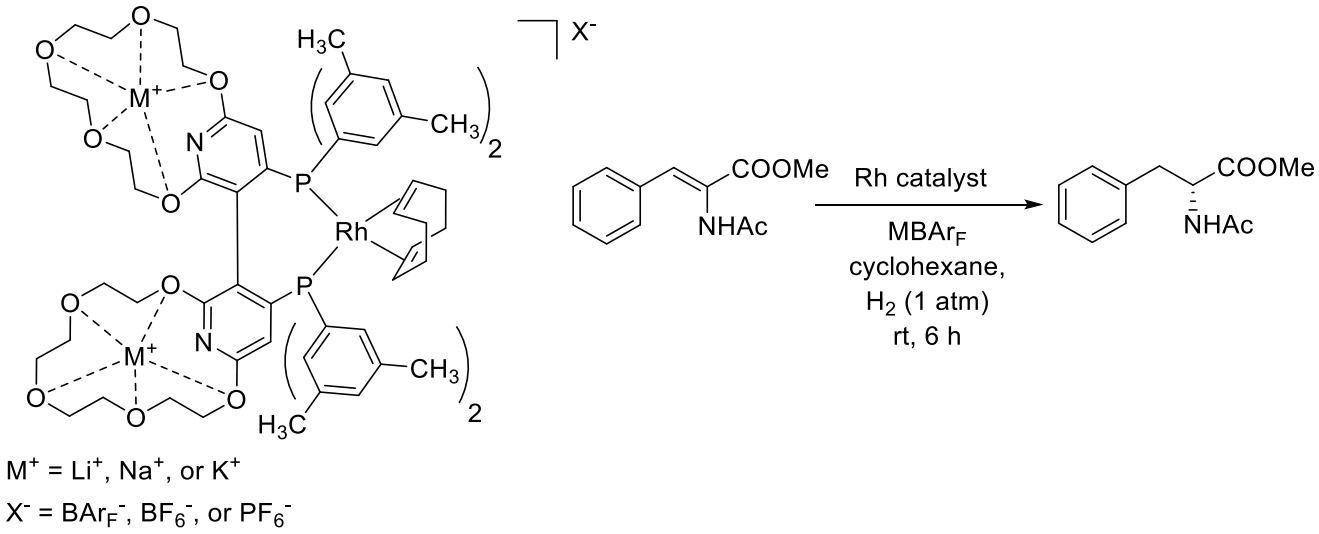

Figure 1.5. Structure of Rh catalyst by Fang and coworkers (left) and its catalytic reaction (right).[5]

Cations and substrate activation

Another way cations can influence transition metals is through substrate activation. This is demonstrated in two different matallocycle molybdenum carbonyl complexes. The first is *cis*-($M(CO)_4[Ph_2P(OCH_2CH_2)_3OPPh_2]$) (Figure 1.6).[15] This metal complex will react with RLi (R = Me, Ph, ^{t}Bu) or Et_2N^- as shown in Figure 1.6.[9] This is in stark contrast to *cis*-$Mo(CO)_4(PPh_3)$ and *cis*-$Mo(CO)_4(PPh_2OMe)_2$ which have no reactivity with RLi (R = Me, Ph, ^{t}Bu) or Et_2N^-. The

reason for the difference in reactivity is due to lithium being attracted to the metallocycle and making the carbonyl more nucleophilic (pulling electron density away). In addition, the Li^+ acts to stabilize the benzoylate-acylate-type oxygen of the product (lowering its energy) and making the reaction as a whole favorable.

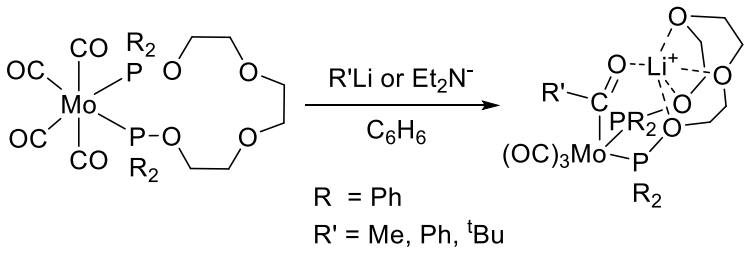

Figure 1.6. Reaction of *cis*-($Mo(CO)_4[Ph_2P(OCH_2CH_2)_3OPPh_2]$) with RLi (R = Me, Ph, ^tB), or Et_2N^-

Similarly, Grey and coworkers reported that the addition of Li^+ caused the carbonyl-metal bonds on the molybdenum complex to weaken (Figure 1.7).[10] They calculated a decrease of approximately 10% in the strength of the back bounding by monitoring the C≡O stretch by FT-IR. Interestingly, the decrease was the same for both *cis* and *trans* carbonyl ligands. They rationalized that the decrease in metal carbonyl bond strength is the result of the lithium cation being bound near the metal center and decreasing its ability to donate electrons into the carbonyl's π* orbitals. A control experiment with a complex not having a metallacrown (*cis*-$Mo(CO)_4\{P(OPh)_3\}_2$) did not see a change in ν_{co} stretch with the addition of $LiB(C_6F_5)_4 \cdot 2Et_2O$, indicating that the metallacrown ether is responsible for changing the CO ligands bond strength on the molybdenum.

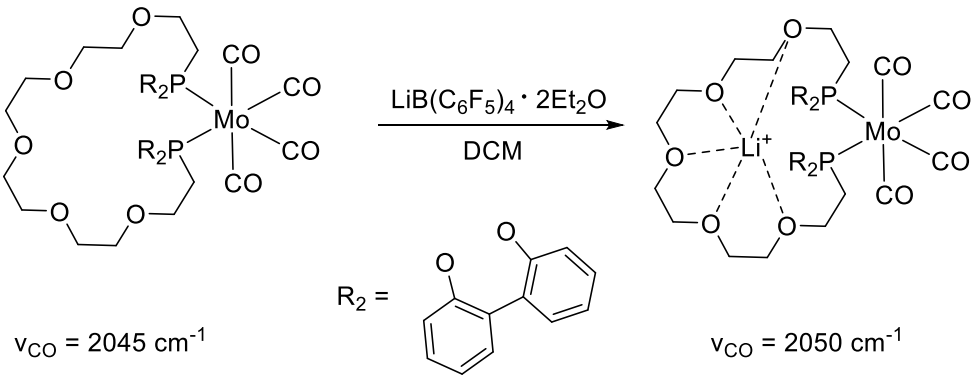

Figure 1.7. Reaction of *cis*-($Mo(CO)_4[Ph_2P(OCH_2CH_2)_6POP(2,2'\text{-}O_2H_8C_{12})_2]$) with $LiB(C_6F_5)_2 \cdot 2\ Et_2O$.

Cations and geometry control

The bite angle is the ligand-metal-ligand bond angle in a bidentate ligand. Changes in this angle can modify the properties of the transition metal.[11] Similarly, switching from *cis* to *trans* isomer results in a complex with different properties. For example, cisplatin is a cancer treatment drug while the *trans* isomer (transplatin) is not (Figure 1.8).[12] In addition, *trans* chelating bisphosphite palladium complexes often produce lower selectivity as catalysts relative to their *cis* isomer.[8] The following sections will discuss how cation-responsive glycol ligands could be used to control bite angle and geometry.

Figure 1.8. Structure of cisplatin (left) and transplatin (right).

Significance of gold oxidative addition

Oxidative addition is a type of reaction in which the oxidation number and the coordination number of a metal center increases. This type of reaction is often involved in the

catalytic cycle of transition metals. Examples of Au(I) oxidative addition, especially of C_{aryl}-halogen bonds and C-C bonds, are relatively rare. Gold(I) is kinetically inert due to its preference for linear configuration, high redox potential (Au(I)/Au(III) E_o = +1.41 V)[13], and relativistic effects (Figure 1.9).[14]

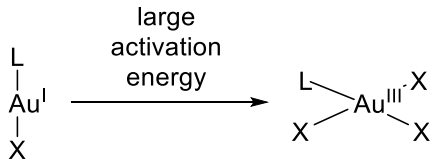

Figure 1.9 Gold(I) is kinetically inert.

Previous work has shown that reducing the bite angle of a Au(I) complex from the typical 180° for a linear Au(I) complex can facilitate oxidative addition of C_{aryl}-halide bonds (Figure 1.10).[15]

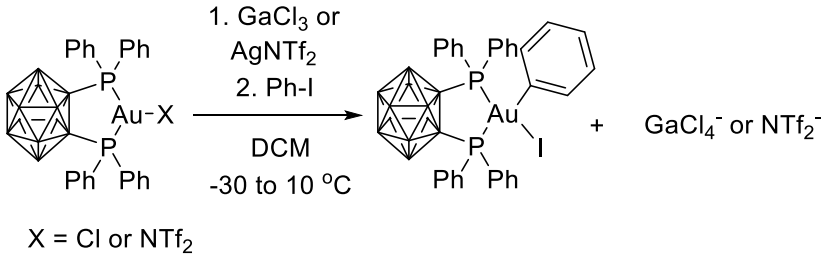

Figure 1.10. Oxidative addition to a bisphosphine gold complex. The phosphines are bound to ortho-carborane.

The approach would be to form a metallocycle with gold and see if inserting a small cation would decrease the bite angle around gold and allow oxidative addition of C_{aryl}-halide bonds to occur (Figure 1.11).

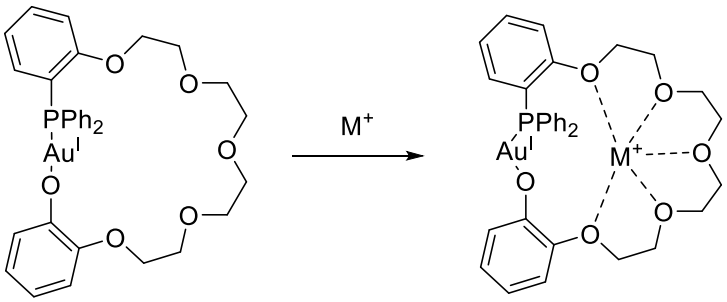

Figure 1.11. Possible route to reduce the activation energy barrier for oxidative addition of Au(I).

The next section will discuss how cations could influence the isomerization of platinum complexes.

Significance of platinum geometry

As noted previously, the geometry of a metal complex can influence its reactivity. An example of the *cis*-*trans* isomerization of $PtCl_2\{Ph_2P(CH_2CH_2O)_3CH_2CH_2PPh_2\text{-}P,P'\}$ is shown in Figure 1.12.[16] The isomerization as monitored by ^{31}P NMR would take place when a drop of 12 M DCl was added to *trans*-$[PtCl_2\{Ph_2P(CH_2CH_2O)_3CH_2CH_2PPh_2\text{-}P,P'\}]$ in D_2O. The isomerization would not occur in 1,2-tetrachloroethane-d_2 in temperatures up to 75 ^oC.

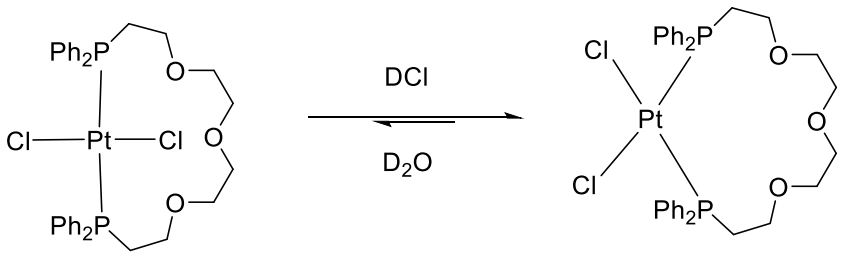

Figure 1.12. *trans*-$[PtCl_2\{Ph_2P(CH_2CH_2O)_3CH_2CH_2PPh_2\text{-}P,P'\}]$ isomerizes to *cis*-$[PtCl_2\{Ph_2P(CH_2CH_2O)_3CH_2CH_2PPh_2\text{-}P,P'\}]$ in the presence of acid.[16]

A question our research is trying to answer is: would the equilibrium of one of the isomers be more favored with the addition of a small cation? A cation may be able to interact more favorably with one isomer over another. In the example shown below, a cation could

interact with both glycol chains in the *cis* conformation but only one glycol chain in the *trans* isomer (Figure 1.13).

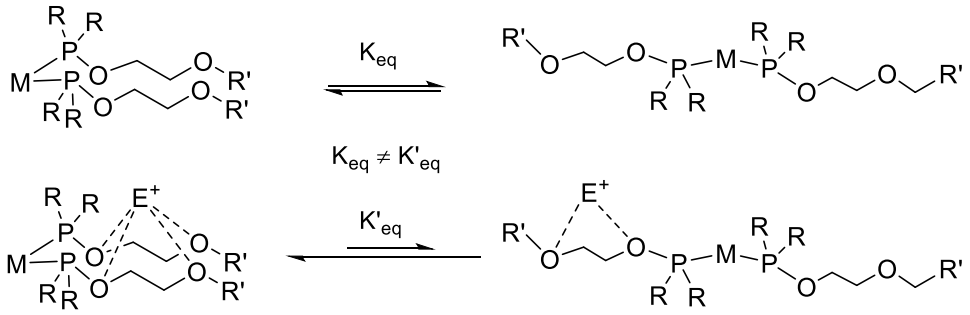

Figure 1.13. Possible equilibrium change with addition of cation (E^+).

This would make the equilibrium shift towards the *cis* isomer when the salt is added. The next chapter will discuss the synthesis of the glycol chain used.

Notes to Chapter 1

[1] Pedersen, C. J. *J. Am. Chem. Soc.* **1967**, *89*, 2495–2496.

[2] Rovira, L.; Fernández-Pérez, H.; Vidal-Ferran, A. *Organometallics* **2016**, *35*, 528–533.

[3] Pizzano, A. *Chem. Rec.* **2016**, *16*, 2599–2622.

[4] Miller, A. J. M. *Dalton Trans.* **2017**, *46*, 11987–12000.

[5] Zhang, X.-C.; Hu, Y.-H.; Chen, C.-F.; Fang, Q.; Yang, L.-Y.; Lu, Y.-B.; Xie, L.-J.; Wu, J.; Li, S.; Fang, W. *Chem. Sci.* **2016**, ***7***, 4594-4599

[6] Song, F.-T.; Ouyang, G.-H.; Li, Y.; He, Y.-M.; Fan, Q.-H. *Eur. J. Org. Chem.* **2014**, *30*, 6713-6719.

[7] Vidal-Ferran, A.; Mon, I.; Bauzá, A.; Frontera, A.; Rovira, L. *Chem. Eur. J.* **2015**, *21*, 11417–11426.

[8] Rovira, L.; Fernández-Pérez, H.; Vidal-Ferran, A. *Organometallics* **2016**, *35*, 528–533.

[9] Powell, J.; Kuksis, A.; May, C. J.; Nyburg, S. C.; Smith, S. J. *J. Am. Chem. Soc.* **1981**, *103*, 5941–5943.

[10] Sheff, J. T.; Lucius, A. L.; Owens, S. B.; Gray, G. M. *Organometallics* **2011**, *30*, 5695–5709.

[11] Miessler, G. L.; Fischer, P. J.; Tarr, D. A. *Inorganic chemistry*; Pearson: Boston, 2014, 547-550

[12] Alderden, R. A.; Hall, M. D.; Hambley, T. W. *J. Chem. Educ.* **2006**, *83*, 728.

[13] Asomoza-Solís, E. O.; Rojas-Ocampo, J.; Toscano, R. A.; Porcel, S. *ChemComm* **2016**, *52*, 7295–7298.

[14] Bartlett, N. *Gold Bull.* **1998**, *31*, 22–25.

[15] Joost, M.; Zeineddine, A.; Estévez, L.; Mallet−Ladeira, S.; Miqueu, K.; Amgoune, A.; Bourissou, D. *J. Am. Chem. Soc.* **2014**, *136*, 14654–14657.

[16] Owens, S. B.; Smith, D. C.; Lake, C. H.; Gray, G. M. *Eur. J. Inorg. Chem.* **2008**, *30*, 4710–4718.

Chapter 2:

Previous phosphine ligands with glycol chains

Ligands are often divided into two groups based on the type of bond they make with a transition metal. If the atom is attached to a transition metal by a coordinate-covalent bond, it is called an L-type ligand. If the atom is attached to a transition metal by an ionic or covalent bond, it is called an X-type ligand. The vast majority of previously reported metallacrown ethers are LL types. In addition, most are symmetrical due to better synthetic accessibility. Some examples of metallacrown ethers with platinum and palladium are shown below (Figure 2.1).

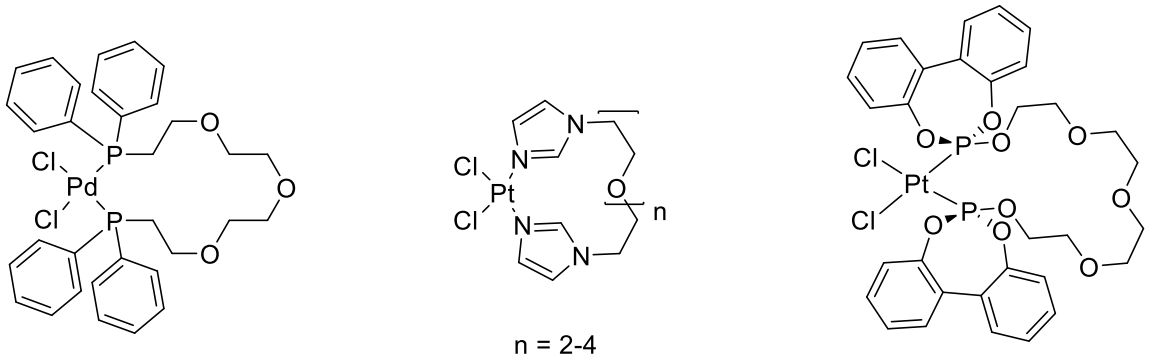

Figure 2.1. Examples of palladium and platinum metallacrown ethers.[1,2]

A rare example of an asymmetric metallacrown ether ligand prepared by Fang and coworkers is shown in Figure 2.2.[3] The synthesis requires 3 steps with only 52% yield in the final step (Figure 2.2).

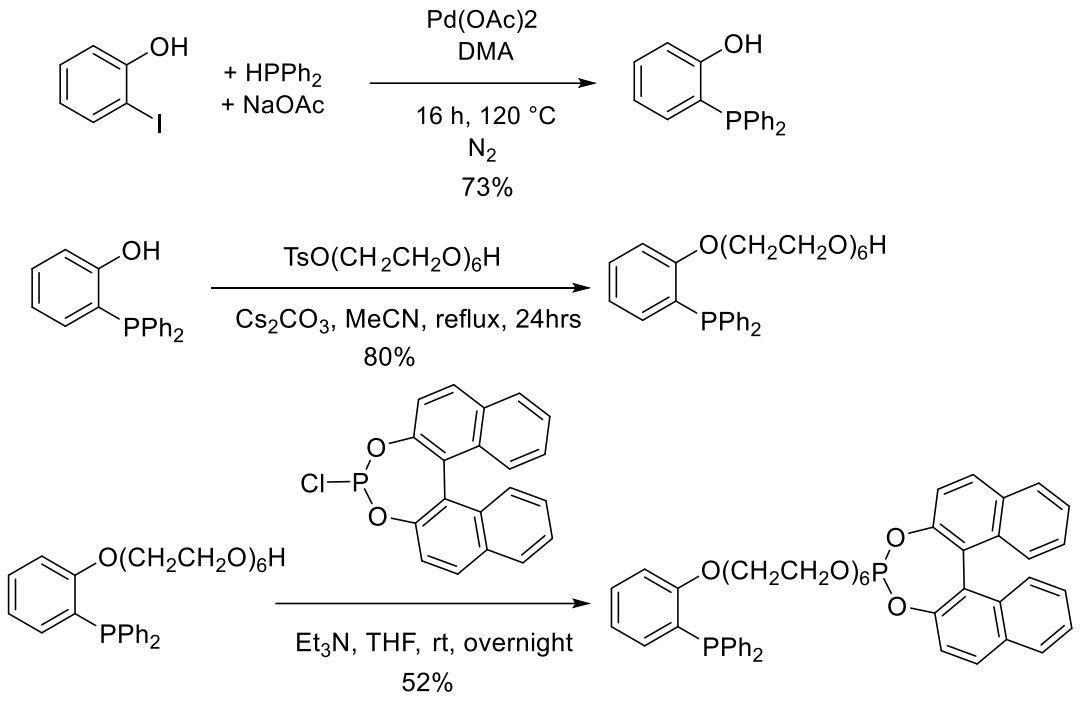

Figure 2.2. Fang and coworkers synthesis of a phosphine-phosphite ligand.[3] Their Rh metal complex is shown in Figure 1.2.

In contrast, many of the symmetric ligands can be made in a 1 step reaction. An example of the synthesis of a bisphosphate ligand is shown in Figure 2.3.

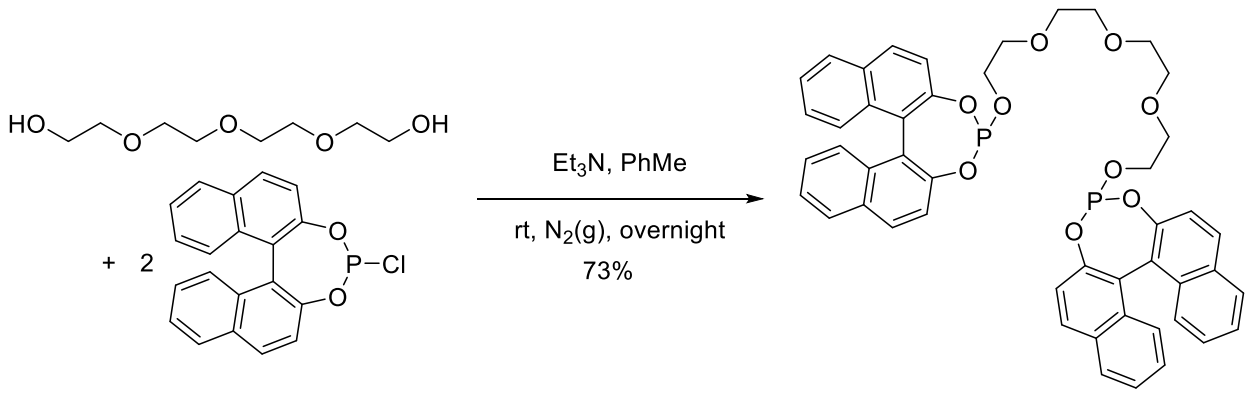

Figure 2.3. Synthesis of bisphosphate ligand by Vidal-Ferran and coworkers. Their palladium metal catalysis is shown in Figure 1.3.

Ligand design consideration for phosphine ligand

As mentioned in chapter 1, previous gold(I) chelating complexes were able to achieve gold(I) oxidative addition of C_{aryl}-halides by reducing the bite angle. The previous models were

LL bidentate ligands on gold, but this has the disadvantage of the metal complex being positively charged. By using an LX ligand, the gold(I) complex would be neutral and could be more susceptible to oxidation. For this reason, and the novelty of these ligands, an LX design was used.

The next choice was what glycol chain length to use. This would determine the size and the number of atoms involved in an eventual metallacrown ether. In addition, the chain length dictates what isomers a metal complex could have. Crystal structures have shown glycol chains of tetraethylene glycol or longer have been shown to span the *cis* and *trans* isomers of platinum complexes so tetraethylene glycol was used for the linker.[4]

The last choice was what atoms would be attached to the metal. For the L-type, we chose a triphenyl phosphine as it would coordinate readily with a late transition metal. For the X-type ligand we wanted an alkoxide to attach to the transition metal. An alcohol would bind to a transition metal as a L-type and need to be deprotonated first to act as an X-type ligand. In addition, the oxygen could not contain β-hydrogens as it could undergo β-hydride elimination.[5] This is especially the case for square planar late transition metals as having only 16 electrons and a coordination number of 4 can accommodate the transition state more readily.[6] A mechanism of this is shown in Figure 2.4. To avoid this problem, the X-type ligand used was a phenoxide as it contains no β-hydrogens.

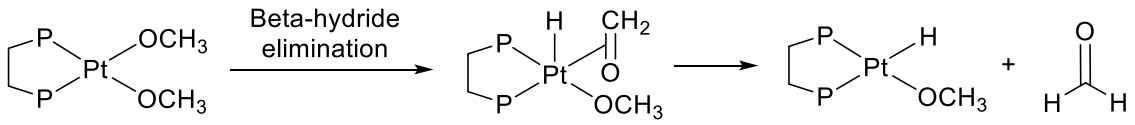

Figure 2.4. β-hydride elimination of methoxide on platinum.

Ligand Synthesis[7]

The structure of ligand target 1 and 2 is shown in Figure 2.5.

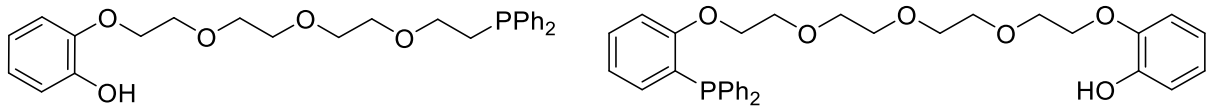

Target 1 Target 2

Figure 2.5. Structure of phosphine ligand target 1 and 2.

An outline of the scheme for target 1 is shown below (Figure 2.6). The first step was a tosylation of one of the alcohol groups. Mono tosylation was accomplished by keeping the concentration of tetraethylene glycol in 10-fold excess.[8] The second step was an S_N2 reaction with a deprotonated catechol serving as the nucleophile to displace the tosyl group. The third step was adding a silyl protecting group to both the phenolic and alkyl alcohols. The forth step was selectively removing the silyl protecting group on the alkyl alcohol.[9]

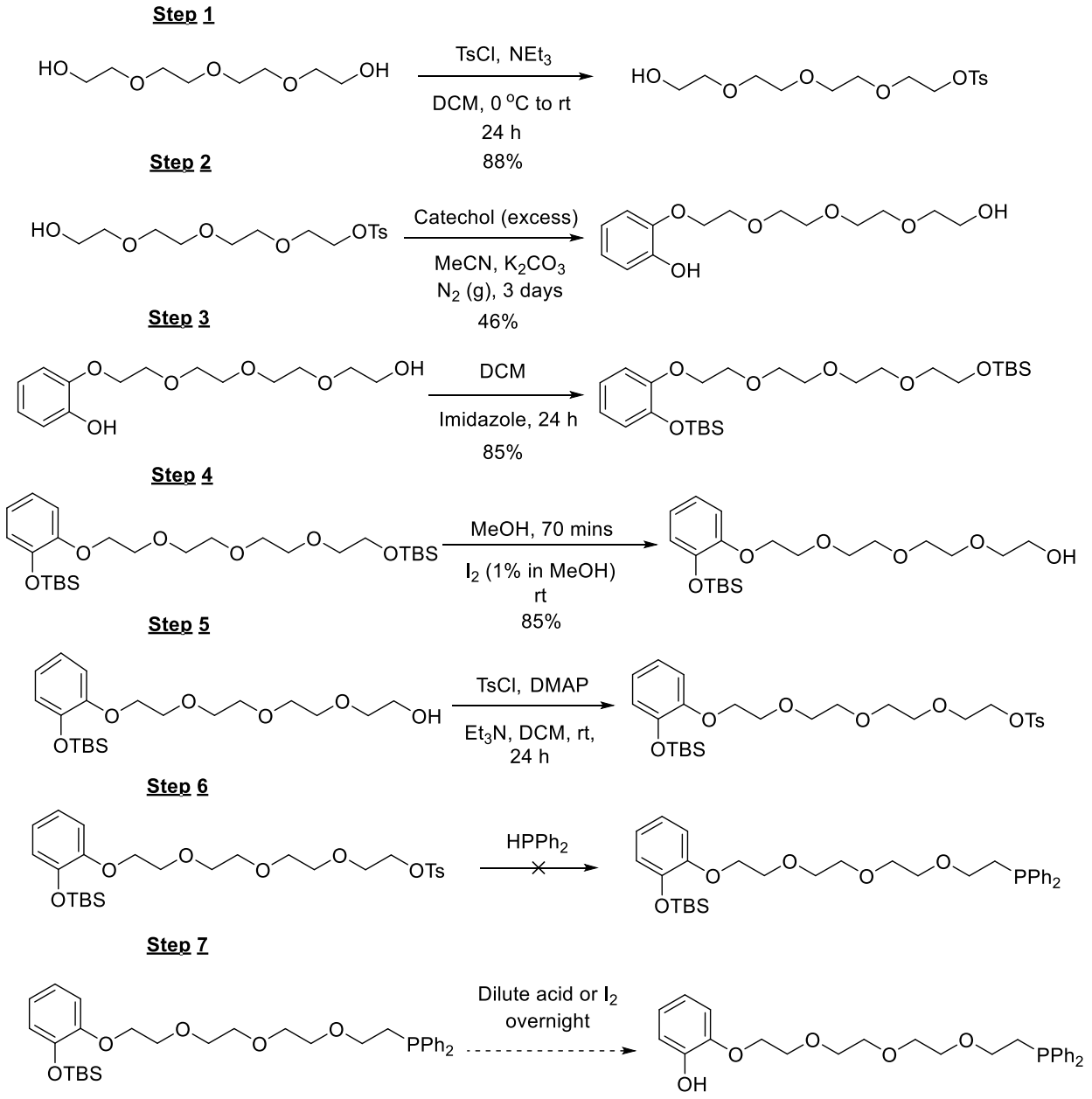

Figure 2.6. Synthetic plan for target 1.

While tosylation in the step one worked well, it was difficult to get the desired product from the tosylation reaction in step five. However, after switching the base to DMAP and following a different procedure, the reaction ran smoothly.

The sixth step was the step that made us abandon this synthetic path. An earlier test showed that the tosyl group could be replaced by diphenyl phosphine (Figure 2.7). This gave us good reason to believe that the reaction would work. However, step six led to a product with peaks in the alkene region, suggesting we did not make the desired product.

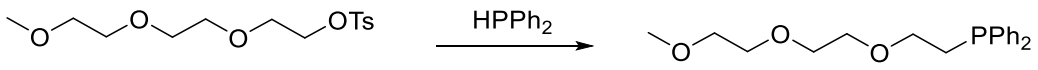

Figure 2.7. Model diphenylphosphine reaction.

At this point, we decided to modify the ligand (target 2, Figure 2.5). The aryl ring would also make the molecule more stable (PPh_3 compounds are usually more stable to water/air compared to $PRPh_2$ compounds). We then planned out two synthetic schemes, Route A (Figure 2.8) and Route B (Figure 2.9).

For both routes, the first step was the same as with the original phosphine ligand (step 1, Figure 2.8 and Figure 2.9). For Route A, the second step was a cross coupling reaction to replace the iodine with a diphenyl phosphine,[10] and the third step was a modification of the condensation step from before from the second step in Figure 2.6.

Literature showed that in order to tosylate phenolic alcohols in the presence of a phosphine, the phosphine must be borane protected (Figure 2.10).[11] The first route had the disadvantage of having to first protect the phosphine with a borane group before tosylation of the alcohol could occur as has been shown by others (step 4, Route A).[11]

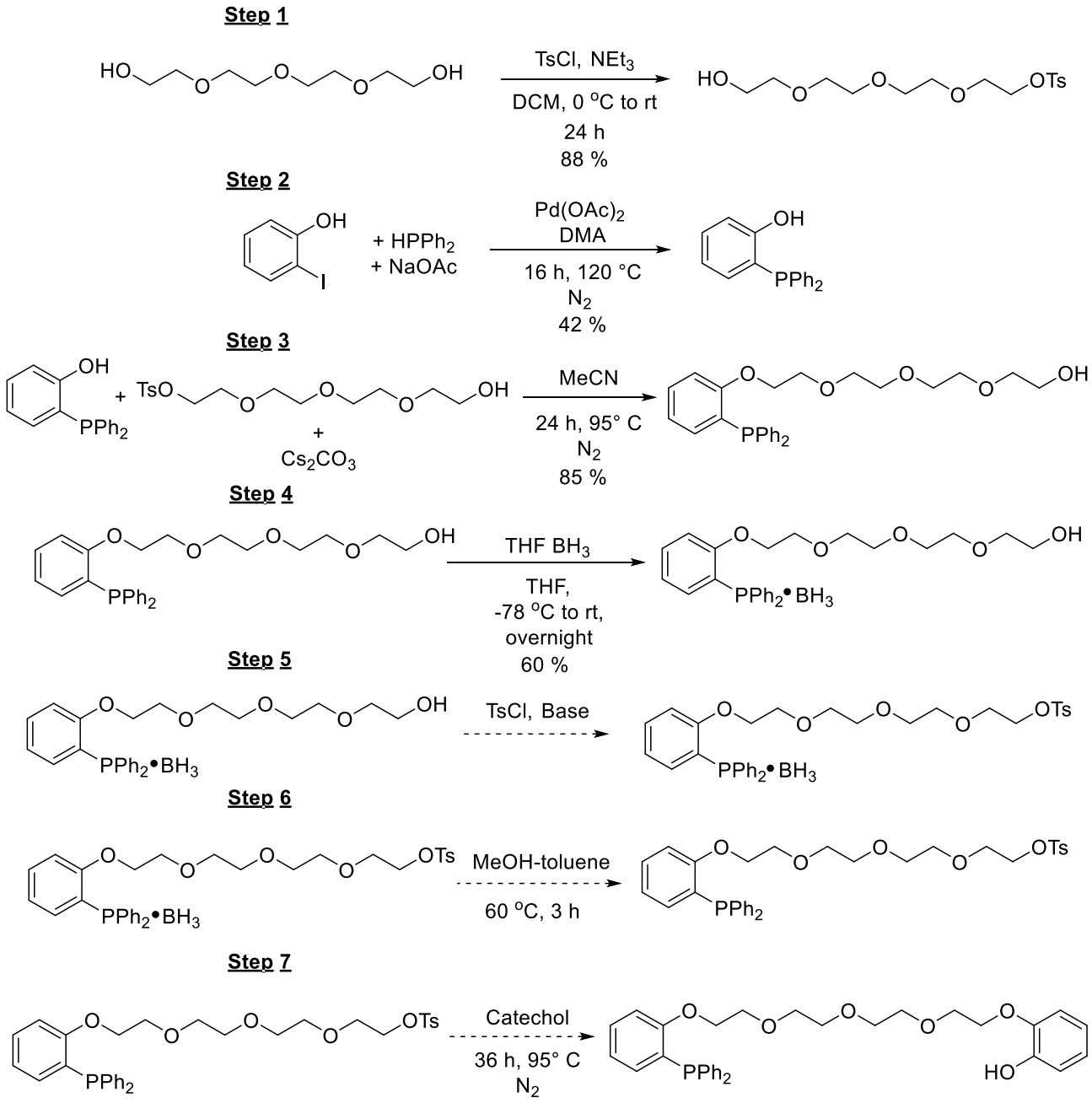

Figure 2.8. Route A to phosphine ligand synthesis in Figure 6.

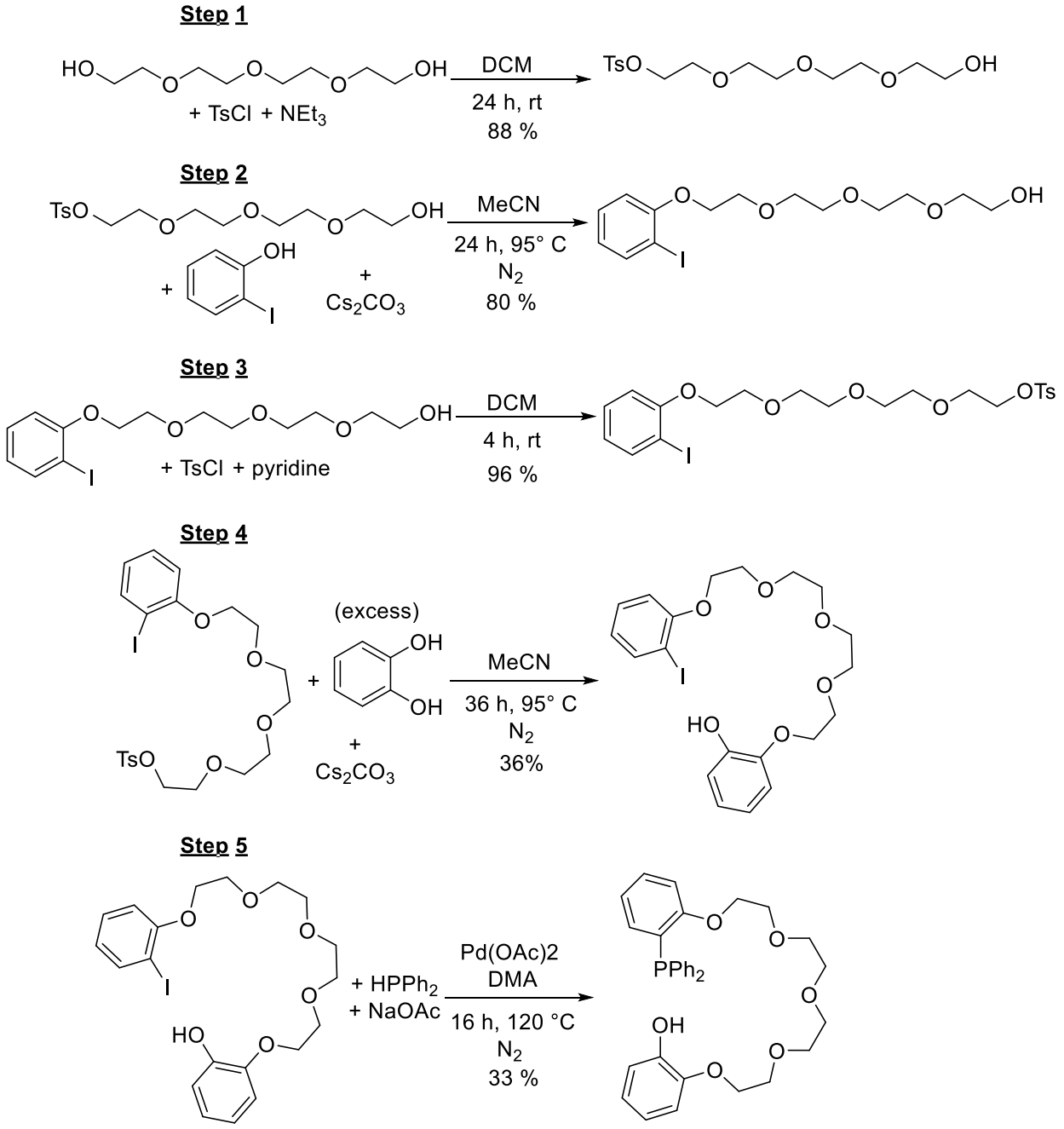

Figure 2.9. Route B to phosphine ligand synthesis in Figure 6.

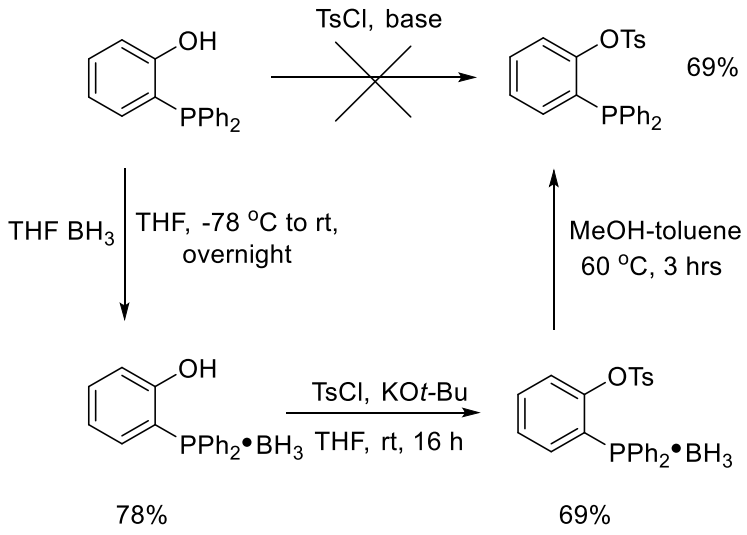

Figure 2.10. Mamat and coworkers method to tosylate in the presence of a phosphine[11]

We attempted a small scale tosylation of the product from step 3 of Route A without a protecting borane to see if this was true for alkyl alcohols as well, but the NMR of the material did not match the desired product. Since this would add 2 extra steps to Route A and the protection, sequential tosylation, and removal of the BH_3 would all require a column, we put this synthetic Route A on hold and decided to focus on Route B (Figure 2.9).

The first step in Route B was the same as Route A with the monotosylation of tetraethylene glycol (step 1, Route B). The next step was a condensation reaction to combine the glycol chain with 2-iodophenol (step 2, Route B).[12] The third was a tosylation of the primary alcohol (step 3, Route B).[13] The fourth step was another condensation reaction with catechol (step 4, Route B). The low yield of pure material was due to a difficult chromagraphic separation and unknown side products being formed. Catechol was used in 6 fold excess to try to prevent some possible side products such as two glycols chains connecting to the same catechol. The fifth step was a cross coupling reaction with palladium that produced the desired phosphine ligand (step 4, Route B).[10] The yield was also low due to similar separation issues and trace

amounts of water in the reaction. Yields improved from 23% to 33% when using more rigorous water-free precautions such as thoroughly drying the reactants on molecular sieves beforehand.

The phosphine ligand was characterized by proton, carbon, and phosphorus NMR (Figure 2.11, Figure 2.12, and Figure 2.13). The proton NMR was consistent with the proposed structure by having 16 protons in the glycol region and 18 in the aryl region (Figure 2.11). Carbon NMR also matched well with 18 aryl peaks and 8 peaks in the ethylene region (Figure 2.12). The phosphorus NMR showed at singlet at -15.5 ppm which is very close to the reported compound diphenyl(2-methoxyphenyl)phosphine which has a peak at -16 ppm in $CDCl_3$ (Figure 2.13).[14]

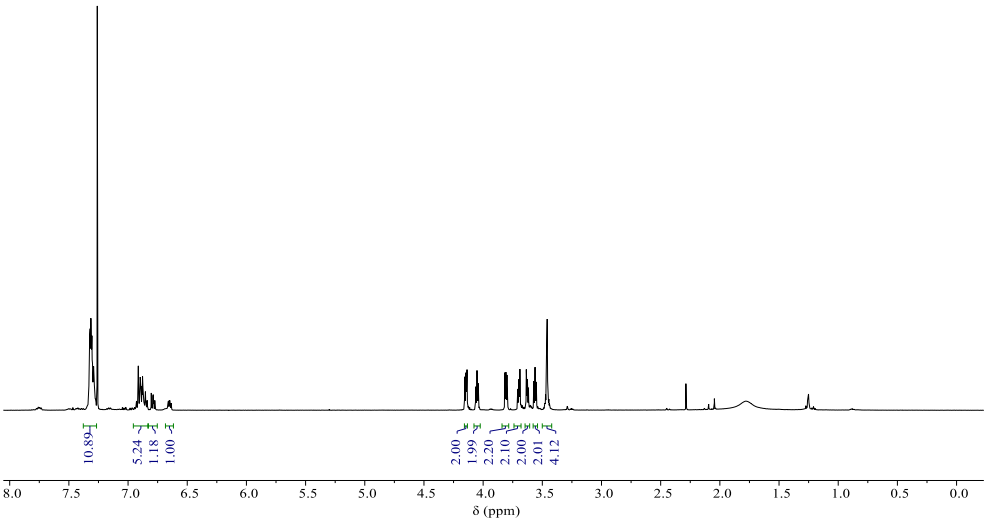

Figure 2.11. ^{1}H NMR of phosphine ligand target 2.

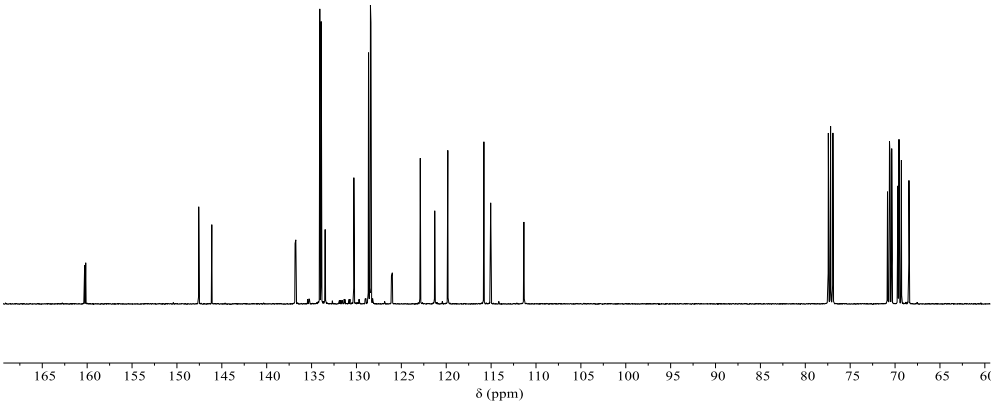

Figure 2.12. ^{13}C NMR of phosphine ligand target 2.

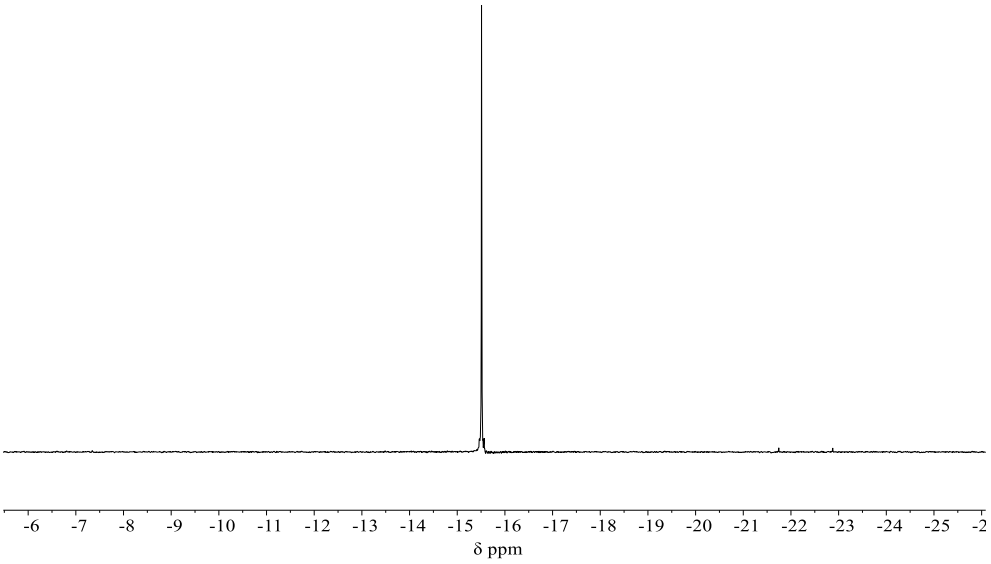

Figure 2.13. ^{31}P NMR of phosphine ligand (δ = -15.5 ppm) target 2.

The five step template we developed could be used to access other similar LX ligands by changing the glycol chain length. In addition, substituents could be added to the benzene rings or

a different phosphine such as di-*tert*-butyl phosphine could be used instead of diphenylphosphine with likely only minor changes to the synthesis plan. The next chapter will present binding studies with the phosphine ligand.

Notes to Chapter 2

[1] Owens, S. B.; Smith, D. C.; Lake, C. H.; Gray, G. M. *Eur. J. Inorg. Chem.* **2008**, *30*, 4710–4718.

[2] Smith, D. C.; Gray, G. M. *Inorg. Chem.* **1998**, *37*, 1791–1797.

[3] Song, F.-T.; Ouyang, G.-H.; Li, Y.; He, Y.-M.; Fan, Q.-H. *Eur. J. Org. Chem.* **2014**, *30*, 6713–6719.

[4] Organo, V. G.; Sgarlata, V.; Firouzbakht, F.; Rudkevich, D. M. *Chem. Eur. J.* **2007**, *13*, 4014–4023.

[5] Ng, S. M.; Zhao, C.; Lin, Z. *J. Organomet. Chem.* **2002**, *662*, 120–129.

[6] Felix, R. J.; Munro-Leighton, C.; Gagne, M. R. *Acc. Chem. Res.* **2014**, *47*, 2319-2331.

[7] Full procedure and characterization are in Chapter 5

[8] Ballardini, R.; Balzani, V.; Dehaen, W.; Dell'Erba, A.; Raymo, F. M.; Venturi, M. *Eur. J. Org. Chem.* **2000**, 591–602.

[9] Lipshutz, B. H.; Keith, J. *Tetrahedron Lett.* **1998**, *39*, 2495–2498.

[10] Ren, G.; Zheng, Q.; Wang, H *Org. Lett.* **2017**, *19*, 2462–2462.

[11] Mamat, C.; Köckerling, M. *Synthesis* **2014**, *47*, 387–394.

[12] Marsden, D. M.; Nicholson, R. L.; Skindersoe, M. E.; Galloway, W. R. J. D.; Sore, H. F.; Givskov, M.; Salmond, G. P. C.; Ladlow, M.; Welch, M.; Spring, D. R. *Org. Biomol. Chem.* **2010**, *8*, 5313.

[13] Elhalem, E.; Bailey, B. N.; Docampo, R.; Ujváry, I.; Szajnman, S. H.; Rodriguez, J. B. *J. Med. Chem.* **2002**, *45*, 3984–3999

[14] Horner, L.; Simons, G. *Phosphorus and Sulfur and the Related Elements* **1983**, *14*, 189–209.

Chapter 3:

Measuring binding constants

The binding affinity of different salts to a crown ether or glycol chains is often calculated and expressed as an equilibrium of bound to non-bound salt.[1] The equilibrium is written in terms of hosts (in this case glycols) and guests (in this case cations) (eq 3.1 and eq 3.2).

$$mH + nG \rightleftharpoons H_m G_n \tag{3.1}$$

$$K_a = \frac{[HG]}{[H][G]} \tag{3.2}$$

One common method for quantifying salt binding is through NMR titration. This method is effective when the binding constant is less than 10^5 M^{-1}.[1] By adding a small known amount of the desired salt to a known amount of a glycol chain, a shift in the NMR spectrum will be observed if there is binding. A shift is seen instead of observing the bound and unbound salt complex because, in general, the association and dissociation of a salt is usually faster than the NMR time scale (≈ms).[2] After adding more and more salt and observing a shift in the NMR, the shift can be correlated with how strongly the salt is binding.

Solving for the binding constant (K_a) is often challenging. All of the values in the equilibrium expression in eq. 3.2 are unknown. The [HG] can't directly be measured due to the fast exchange rate of binding and unbinding of cations. The [H] can't be measured for the same reason as the [HG] and only the initial concentration of host ($[H]_o$) is known. The [G] doesn't give a distinct NMR signal so is also unknown. However, using the mass balance equations of [H] (eq 3.3) and [G] (eq 3.4) yields a new expression for K_a (eq 3.5).Solving for [HG] yields a quadratic equation with unknowns K_a and [HG] (eq. 3.6).

$$[H]_0 = [H] + [HG] \tag{3.3}$$

$$[G]_0 = [G] + [HG] \tag{3.4}$$

$$K_a = \frac{[HG]}{([H]_0 - [HG])([G]_0 - [HG])} \tag{3.5}$$

$$[HG] = \frac{1}{2}\left(G_0 + H_0 + \frac{1}{K_a}\right) - \sqrt{\left(G_0 + H_0 + \frac{1}{K_a}\right)^2 + 4[H_0][G_0]} \tag{3.6}$$

Since the change in the NMR chemical shift (Δδ) is proportional to the mole fraction of [HG] multiplied by some constant (eq 3.7), eq 3.6 can be rewritten as eq 3.8. This equation has 3 unknowns, but something that can be measured (Δδ). Using a program such as BindFit,[1] a non-linear regression can be fit to the titration of data.

$$\Delta\delta = \delta_{\Delta HG}\left(\frac{[HG]}{[H]_0}\right) \tag{3.7}$$

$$\Delta\delta = \frac{\delta_{\Delta HG}}{[H]_0}\left(\frac{1}{2}\left\{\left([G]_0 + [H]_0 + \frac{1}{K_a}\right) - \sqrt{\left([G]_0 + [H]_0 + \frac{1}{K_a}\right)^2 + 4[H]_0[G]_0}\right\}\right) \tag{3.8}$$

The main factors determining what cation will bind most strongly are the size of the crown, the size of the cavity, and the number of oxygen atoms available to donate electron density. Table 3.1 summarizes the four most common crown ether sizes and the cations they prefer.[3] The cavity size can vary, however, by substituents attached or if there is strain on the molecule. In addition, even cations too big/small for a crown will usually still bind. For example,

15-crown-5 will bind K^+ in the absence of sodium and even surround a K^+ cation in a 2:1 stoichiometry if there is excess glycol.[8]

Table 3.1. Common crown ethers and the cations they prefer.

Cation	Ion diameter (Å)	Crown ether	Cavity diameter (Å)
Li^+	1.36	12-crown-4	1.2-1.5
Na^+	1.94	15-crown-5	1.7-2.2
K^+	2.66	18-crown-6	2.6-3.2
Cs^+	3.34	21-crown-7	3.4-4.3

The solvent used can play a significant role in how tightly a metal binds as salts can also interact with the solvent. For example, the binding constant of K^+ to 18-crown-6 was over 500,000 M^{-1} in acetonitrile and methanol, but only 15,000 M^{-1} in DMF and 2,239 M^{-1} in DMSO.[4] Generally, when changing to a more coordinating solvent (such as dichloromethane to THF or acetonitrile), a decrease in the binding constant of approximately 3 orders of magnitude is observed.[5] This is because the solvent is competing with the glycol chain or crown ether for the salt. The solubility of the salt in the solvent can also play a factor as too low a solubility can make it impossible to reach the inflection point of the titration and get a binding constant.[6]

Binding between free phosphine ligand and cations

As mentioned earlier, we had strong reason to believe the phosphine ligand and its corresponding metal complexes would be able to bind small cations to its polyethylene glycol chain. The ligand should not bind cations as tightly as crown ethers due to the macrocycle effect.[7] This is because the entropic cost is much larger for a glycol chain than for a crown ether.

For example, the binding constant of K^+ to 18-crown-6 is 6000 times stronger than its open-chained equivalent in anhydrous methanol (Figure 3.1).[8]

Figure 3.1. Binding constant of K^+ 18-crown-6 (left) and pentaethylene glycol dimethyl ether in dry MeOH.

Based on the size and number of oxygen atoms in the phosphine ligand, we expected either Li^+ or Na^+ to bind the most strongly. These binding studies would tell us how strongly the ligand was binding a cation and what type of binding motif was present. The most common types of binding modes are 1:1, 1:2, and 2:1 host-guest (ligand-salt). An example of these on the phosphine ligand is shown in Figure 3.2. Previous work of cation binding to open chain glycols shows 1:1 binding in the vast majority of glycol chains, salts, and solvents.[9]

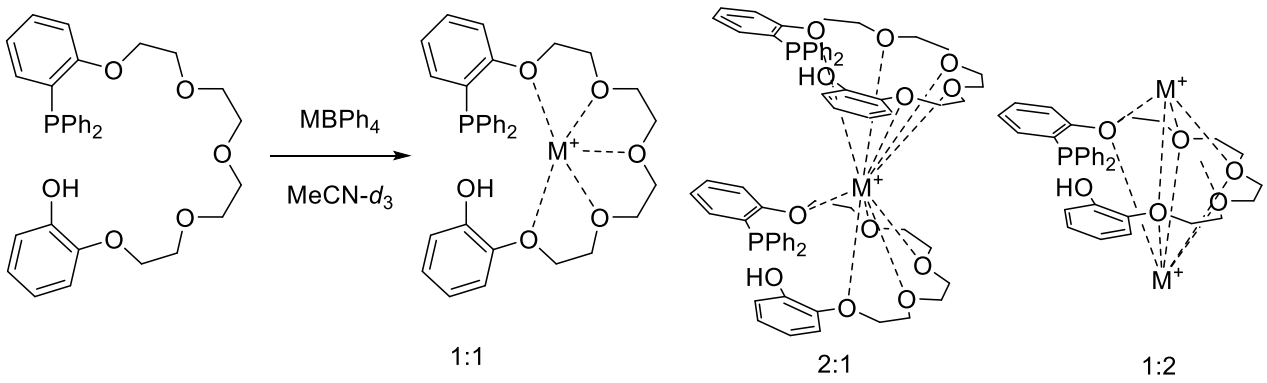

Figure 3.2. Three possible binding motifs for a cation interacting with the phosphine ligand.

For our salts, we chose $NaBPh_4$, $KBPh_4$, and $LiBPh_4 \cdot 3CH_3O(CH_2CH_2)OCH_3$ to get a variety of cation sizes with a common non-coordinating anions. It is also more economical than using the most non-coordinating anionic salts such as the BArF salts.

The binding studies were monitored by proton NMR. Resonance shifting was expected to occur upon binding of the cation to the glycol chain.[10] Binding of salts to similar glycol chains has been shown to be dynamic on the NMR timescale and so no new peaks were expected to be observed, just shifting of the protons in the glycol chain.

Deuterated benzene was originally tried for monitoring cation binding. However, the tetraphenylborate salts have very low solubility in benzene. This made the process much more time consuming trying to get the salt to fully dissolve. In addition, a brown oil precipitated out of solution in the NMR tube after adding only 0.5 equivalents of $NaBPh_4$. These results caused us to change the solvent we used to acetonitrile, which had the advantage of salts being very soluble in it. In addition, it is a common solvent others have used to quantify binding of cations in crown ethers.

After drying the NMR solvent and the phosphine ligand overnight on molecular sieves, a solution of the salts and a solution of the phosphine ligand were prepared. A small amount of anhydrous DCM was added before each titration to use as an internal reference.

Titration of $NaBPh_4$ into an NMR tube containing phosphine ligand in MeCN-d_3 caused shifts in the NMR spectrum. The greatest shift was seen in the alkyl region, which is to be expected as they are the closest protons to where the cation would bind. A stack plot of the titration is shown in Figure 3.3.

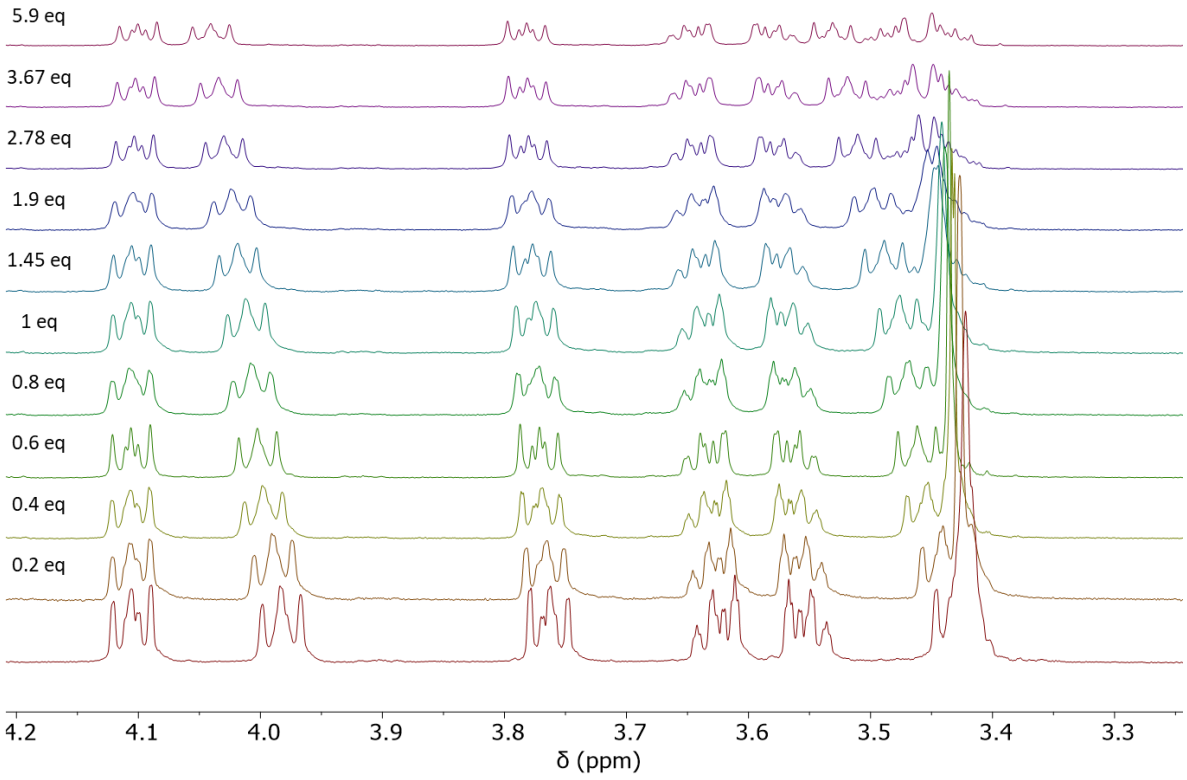

Figure 3.3. NMR titration of phosphine ligand with $NaBPh_4$ in MeCN-d_3.

Using the program Bindfit,[11,12] we were able to fit the data to different types of host-guest (glycol-cation) binding systems. In choosing which protons to track the changes of the NMR resonance, we picked protons that showed large movement and were not overlapping with other protons. We chose to use the triplet at 3.98 ppm to monitor the cation binding in all of the salts. Previous work has shown that this proton is in the middle of the glycol chain.[13] This is ideal since small amounts of water could, in theory, interact with the cation binding of protons near the end of the glycol chain but would not influence the peaks near the middle of the glycol chain. Inputs of the proton NMR shift with the concentration of the salt and phosphine ligand fit best to a 1:1 binding system. Binding constant was calculated to be 133 M^{-1} and 119 M^{-1} in two trials (Table 3.2).

Table 3.2. Binding constant of cation to Phosphine ligand

Salt	Binding constant (M^{-1})	% Error[a]	Binding mode
Li^+	45	± 7.2 %	1:1
Li^+	54	± 10.5 %	1:1
Li^+	44	± 10.0 %	1:1
Na^+	133	± 4.4 %	1:1
Na^+	119	± 3.4 %	1:1
K^+	14	± 20.2 %	1:1
K^+	17	± 11.7 %	1:1

a 95% confidence integral.

Following the same proton signal at 3.98 ppm, we observed a shift in the NMR resonance with the addition of $LiBPh_4 \cdot 2Et_2O$. The binding also fit well with a 1:1 host-guest binding model. For lithium, we calculated a slightly weaker interaction than sodium with binding constants of only 44, 45, and 54 M^{-1} in three trials. This result was expected as lithium can only accommodate 4 oxygen donors and our phosphine ligand has 5 ethylene oxygen atoms, one phenolic oxygen, and a phosphine atom that could all in theory have a favorable interaction with a cation. If the lithium cation cannot accommodate all of the donors, then we would expect the shift in resonance to be smaller, as is observed. Stack plot of the NMR titration is shown in Figure 3.4.

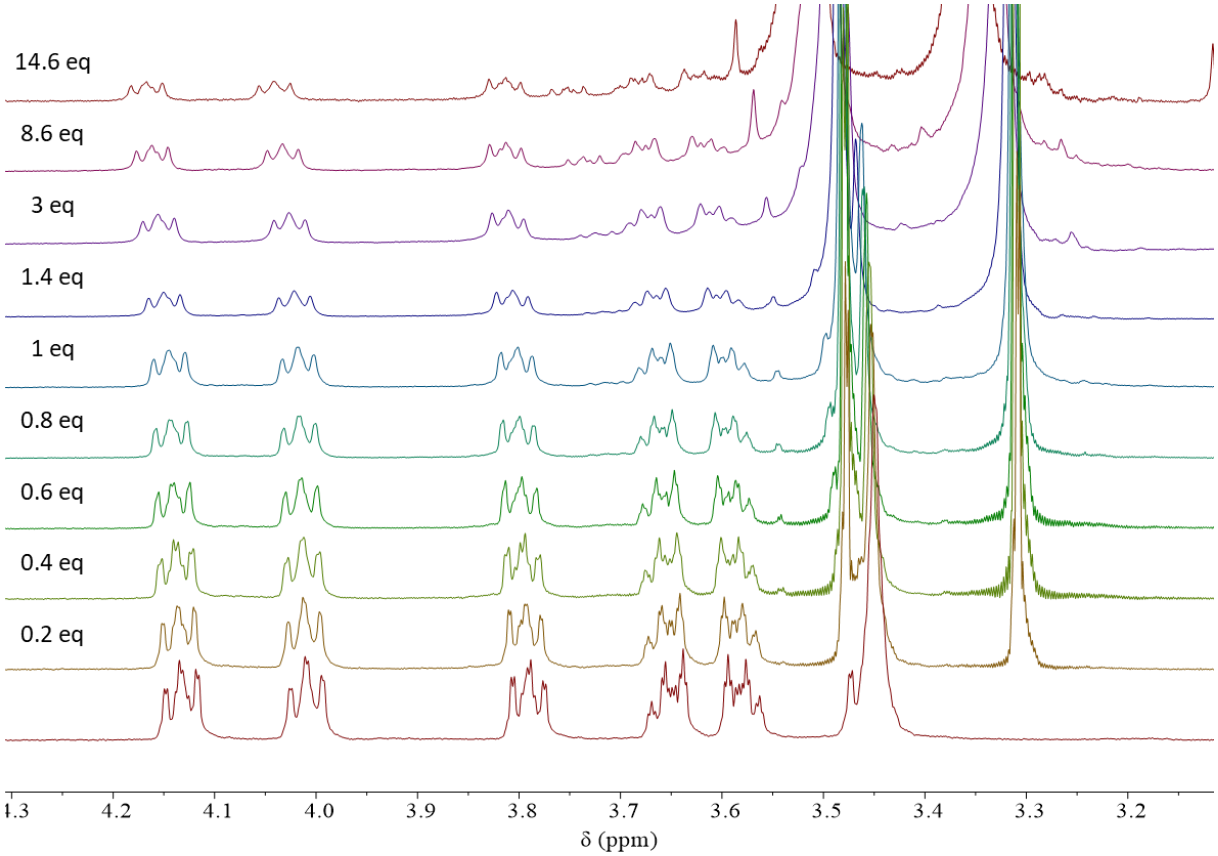

Figure 3.4. NMR titration of phosphine ligand with $LiBPh_4 \cdot 3$(1,2-Dimethoxyethane).

The last salt used was $KBPh_4$. We again observed shifting in the NMR resonances with the titration of the salt. Being much larger than the other cations, we expected the potassium cation to not bind as tightly to the phosphine ligand. The proton NMR of the titration is shown in Figure 5. The 1:1 binding model again fit best, but the error is much higher than previous salts (Table 3.2). There are a couple of possible reasons for this. The first is the salt has a much lower solubility than the other salts. This required having to add $KBPh_4$ as a weighed solid to get to high equivalent values and would not be as consistent as micro pipetting from a solution. Another possible reason is even though other binding models tested (1:2 and 2:1) gave even greater error, it is possible another binding system is the true stoichiometry of the binding. In addition, a more complicated binding system (such as a mixture of different binding interactions)

could be happening. While this is unlikely based on previous work of cation binding in polyethylene glycols,[9] it cannot be completely ruled out.

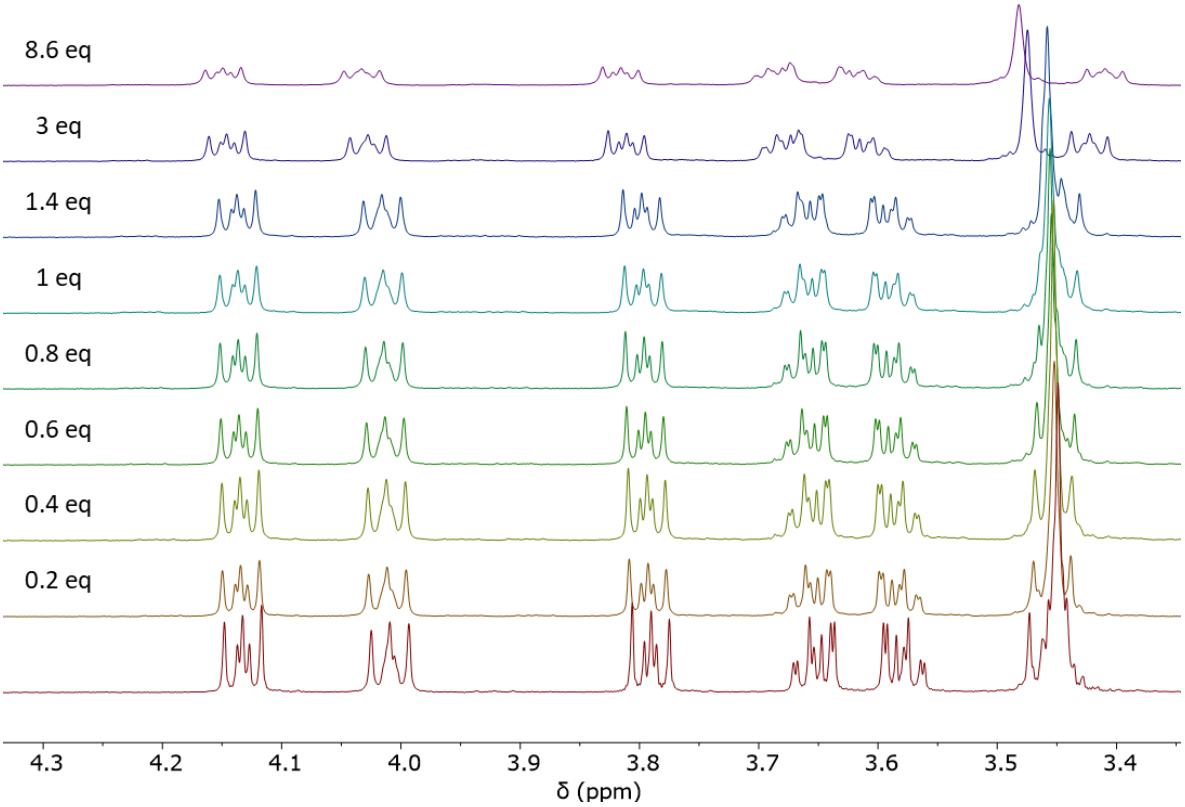

Figure 3.5. NMR titration of phosphine ligand with $KBPh_4$ in MeCN-d_3.

Notes to Chapter 3

[1] P. Thordarson, *Chem. Soc. Rev.* **2011**, *40*, 1305-1323.

[2] Bryant, R. G. *J. Chem. Ed.* **1983**, *60*, 933.

[3] Cai, Z.; Do, L. H. *Organometallics* **2017**, *36*, 4691–4698.

[4] Solovev, V. P.; Strakhova, N. N.; Raevsky, O. A.; Rüdiger, V.; Schneider, H.-J. *J. Org. Chem.* **1996**, *61*, 5221–5226.

[5] Smith, J. B.; Kerr, S. H.; White, P. S.; Miller, A. J. M. *Organometallics* **2017**, *36*, 3094–3103.

[6] Martin, J. R.; Lucius, A. L.; Gray, G. M. *Organometallics* **2015**, *34*, 4605–4617.

[7] Inoue, Y. *Cation binding by macrocycles*; Marcel Dekker: New York, N.Y, 1990; 253–310.

[8] Gokel, G. W. *Crown ethers and cryptands Monographs in Supramolecular Chemistry*; RSC: Cambridge, 1991; 64–98.

[9] Yanagida, S.; Takahashi, K.; Okahara, M. *Bull. Chem. Soc. Jpn.* **1978**, *51*, 3111–3120.

[10] Sawada, K.; Imai, A.; Satoh, K.; Kikuchi, Y. *J. Phys. Chem. B* **2007**, *111*, 4361–4367.

[11] http://supramolecular.org (accessed May 24, 2019).

[12] D. Brynn Hibbert and Pall Thordarson, *Chem. Commun.* **2016**, *52*, 12792-12805.

[13] Sawada, K.; Imai, A.; Satoh, K.; Kikuchi, Y. *J. Phys. Chem. B* **2007**, *111*, 4361–4367.

Chapter 4:

Synthesis of platinum complexes[1]

With the phosphine ligand in hand, the next goal was to put the ligand on a metal. Before pursuing gold complexes, platinum was used as a model metal. Approximately 33% of platinum is NMR active (^{195}Pt) and so the reactions would be easier to monitor by ^{31}P NMR as the P-Pt coupling constant will vary based on what other ligands are attached to the platinum. In addition, a phosphorus peak with no satellites would give us clear evidence that the phosphine is not attached to platinum.

L_2PtCl_2 (L = phosphine ligand)

When $PtCl_2(NCPh)_2$ is stirred with 2 equivalents of the phosphine ligand in DCM, the *trans* platinum chloride product readily forms (Figure 4.1). The *trans* isomer was confirmed based on the P-Pt coupling constant from literature (Table 4.1).[2] The compound then slowly equilibrates with the *cis* isomer after sitting in a DCM solution for several days (Figure 4.2 and Figure 4.3) as monitored by ^{31}P NMR. The *trans* isomer can be isolated with column chromatography using 1:1 DCM/EtOAc.

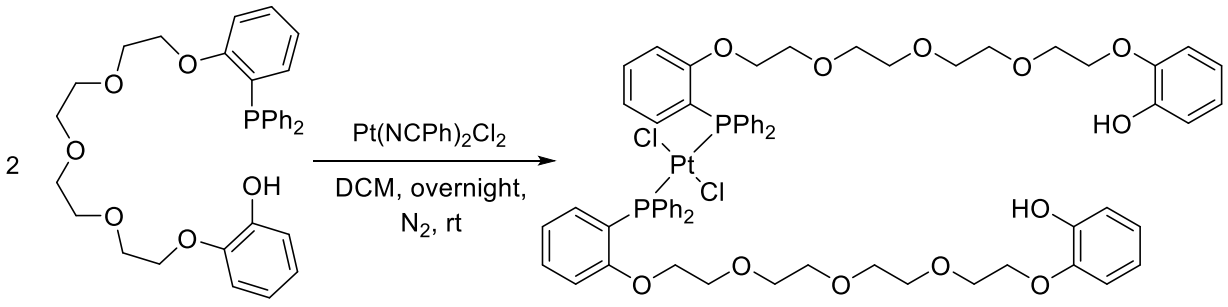

Figure 4.1. Formation of Pt(phosphine ligand)$_2$Cl$_2$.

Table 4.1. Phosphorus NMR resonance and coupling constants of platinum chloride complexes.

Compound	^{31}P Chemical Shift[a]	$J_{P\text{-}Pt}$[a]
trans-$PtCl_2(PPh_3)_2$	17.3 ppm[2]	2560 Hz[2]
cis-$PtCl_2(PPh_3)_2$	12.0 ppm[2]	3677 Hz[2]
trans-$PtCl_2$(phosphine ligand)$_2$	13.9 ppm	2698 Hz
cis-$PtCl_2$(phosphine ligand)$_2$	8.46 ppm	3801 Hz

[a] in $CDCl_3$

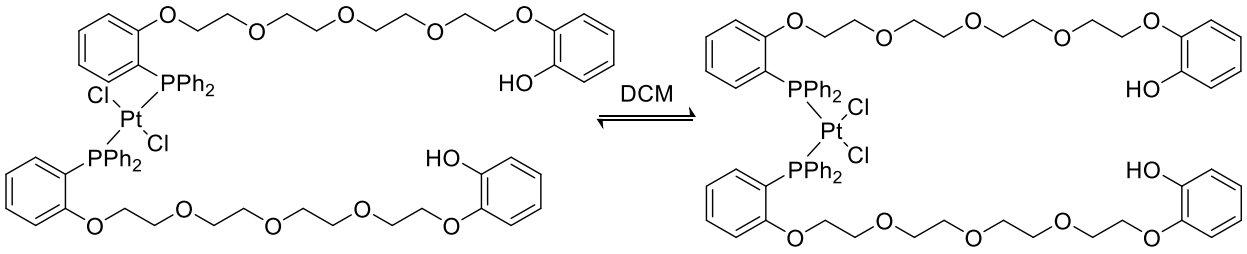

Figure 4.2. Isomerization of *trans*-$PtCl_2$(phosphine ligand)$_2$ to *cis*-$PtCl_2$(phosphine ligand)$_2$.

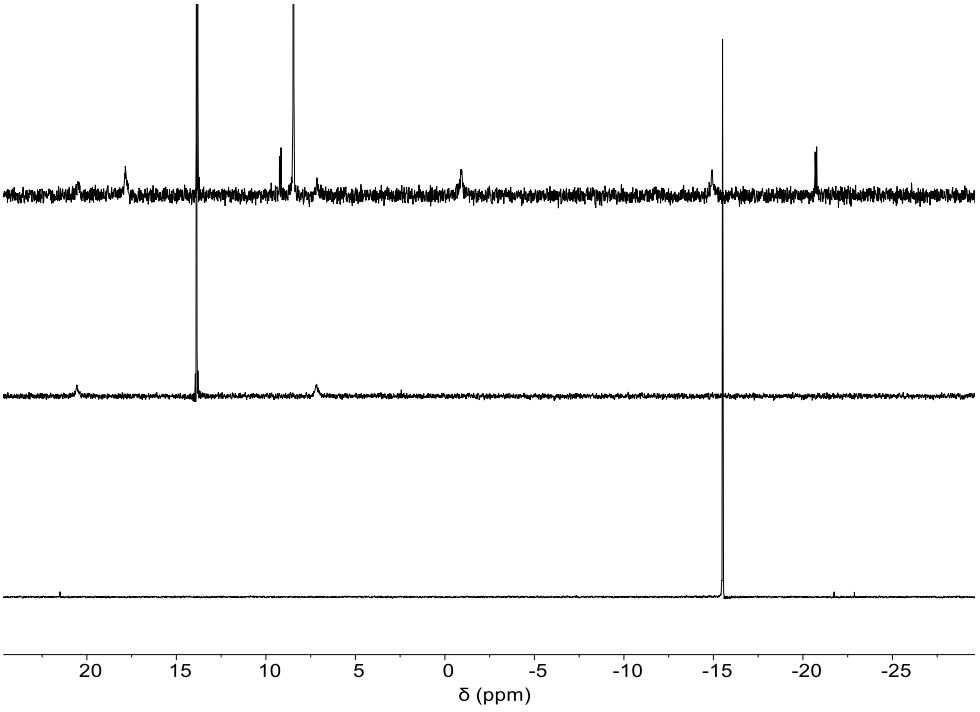

Figure 4.3. ^{31}P NMR showing the conversion of the free phosphine ligand (bottom) to *trans*-Pt(phosphine ligand)$_2Cl_2$ (middle, $J_{P\text{-}Pt}$ = 2698 Hz) and to a mixture of *cis* and *trans* isomers (top, *cis*-Pt(phosphine ligand)$_2Cl_2$ $J_{P\text{-}Pt}$ = 3801 Hz)

L_2PtMe_2 (L = phosphine ligand)

Platinum methyl complexes with the phosphine ligand were also synthesized. The precursor for this reaction was synthesized in a two-step process. First, K_2PtCl_4 was reacted with diethyl sulfide in water under argon to generate $PtCl_2(SEt_2)_2$ (Figure 4.4). After extracting the product with DCM and drying the product, the platinum compound was treated with methyl lithium from a literature procedure to produce $[PtSEt_2Me_2]_2$ after crystallization from acetone (Figure 4.4).[3] The Pt complex was then reacted with the phosphine ligand in toluene to yield the methyl version of the platinum complex (Figure 4.5). It was identified to be the *cis* isomer by ^{31}P NMR based on its $J_{P\text{-}Pt}$ value of 1940 Hz (*cis*-$Me_2Pt(PPh_3)_2$ which appears at 27.7 ppm with $J_{P\text{-}Pt}$ = 1900 Hz in CD_2Cl_2)[4] (Figure 4.6).

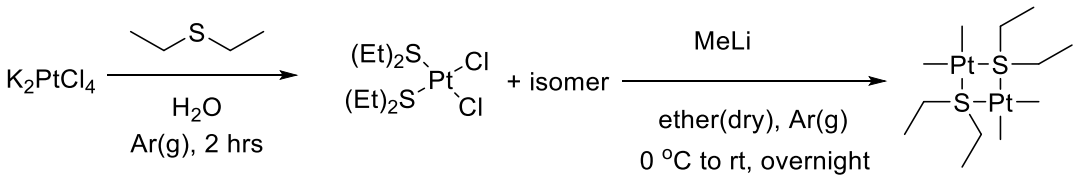

Figure 4.4. Formation of $[PtSet_2Me_2]_2$

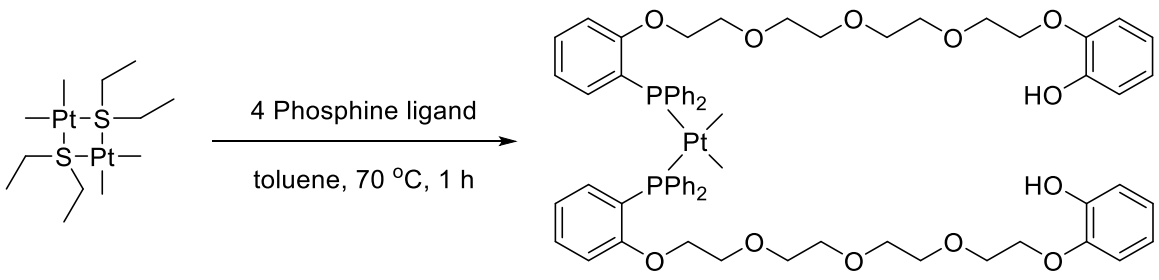

Figure 4.5. Formation of *cis*-$Me_2Pt(\text{phosphine ligand})_2$.

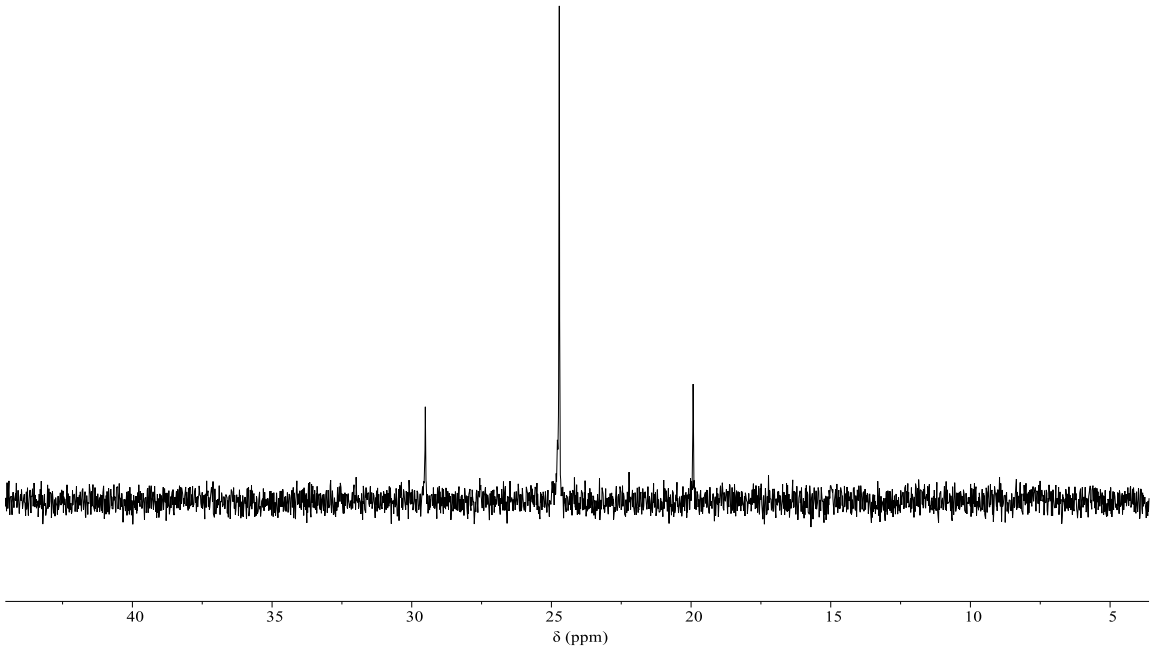

Figure 4.6. ^{31}P NMR of *cis*-$Me_2Pt(phosphine\ ligand)_2$

Cyclometalating the phosphine ligand on platinum

With $Cl_2Pt(phosphine\ ligand)_2$ and $Me_2Pt(phosphine\ ligand)_2$ in hand, the next step was to cyclometalate the phosphine ligand on platinum. First attempts included the addition of an organic base to $Cl_2Pt(phosphine\ ligand)_2$ based on previous work showing trimethylamine and DBU (1,8-diazabicyclo[5.4.0]undec-7-ene) were able to create Pt-phenoxide bonds (Figure 4.7 and Figure 4.8).[5,6]

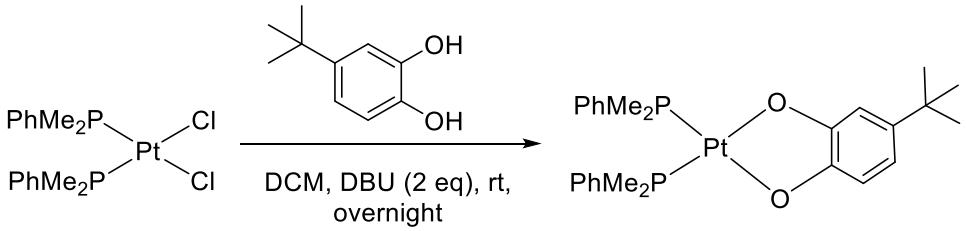

Figure 4.7. Formation of Pt-O bond with DBU.[5]

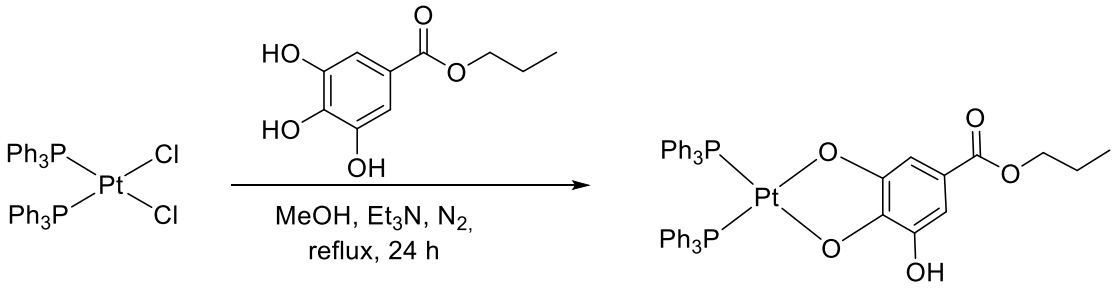

Figure 4.8. Formation of Pt-O bond with trimethylamine.[6]

The idea was to deprotonate the phenol on the end of the phosphine ligand, which could then displace the chloride and attach to the platinum center (Figure 4.9).

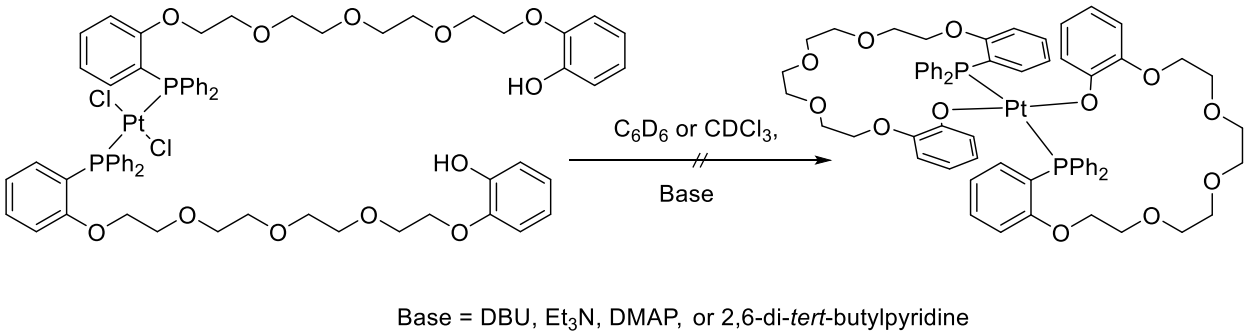

Figure 4.9. Cyclometalation attempts of *trans*-Cl_2Pt(phosphine ligand)$_2$ with DBU, Et_3N, DMAP, or 2,6-di-*tert*-butylpyridine in C_6D_6 or $CDCl_3$

Bases such as NEt_3, 4-dimethylaminopyridine, DBU (1,8-diazabicyclo[5.4.0]undec-7-ene), and 2,6-di-*tert*-butylpyridine were used but did not lead to the desired product. ^{31}P NMR of the reaction of Cl_2Pt(phosphine ligand)$_2$ with DBU in C_6D_6 is shown below (Figure 4.10). The peaks at -15.5 and 13.8 ppm corresponded to free phosphine ligand and *trans*-Cl_2Pt(phosphine

ligand)$_2$ respectively. The largest peak was seen at 23.1 ppm and had no platinum satellites, perhaps corresponding to a phosphine oxide (triphenylphosphine oxide appears at 24.4 ppm in C_6D_6).[7] The sterically hindered base 2,6-di-*tert*-butylpyridine did not give free ligand but left some starting material and the same peak at 24.4 ppm.

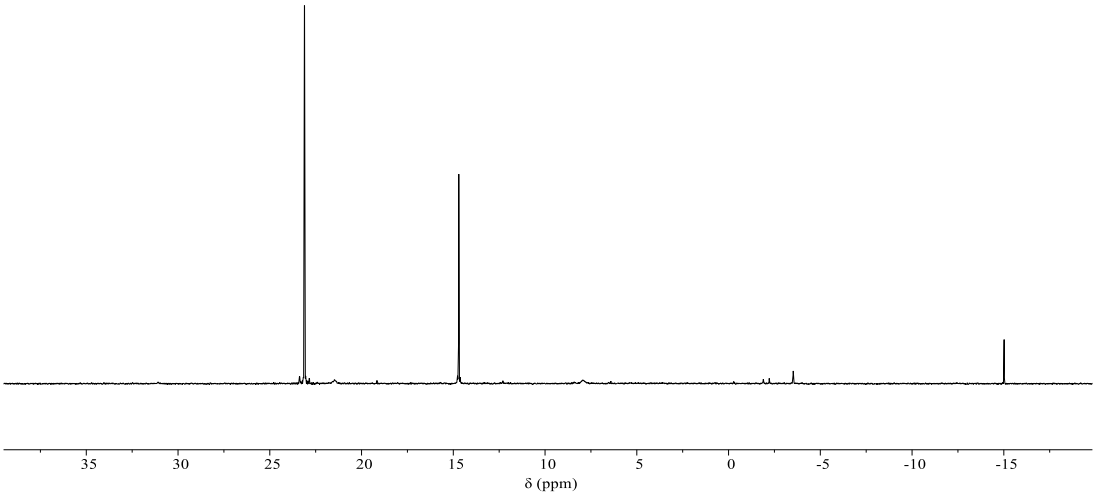

Figure 4.10. ^{31}P NMR of *trans*-Cl_2Pt(phosphine ligand)$_2$ with DBU in C_6D_6.

Another method using carbonate salts was then attempted. The rationale was using Ag_2CO_3 would lead to the formation of CO_2 (g) and AgCl (which would precipitate out of solution as a solid) which would drive the reaction forward.[8,9] Heinicke and coworkers showed a similar method worked with other carbonate salts such as K_2CO_3 to cyclometalate a phenoxide group on palladium (Figure 4.11).[10] The results of Ag_2CO_3 led to a large mixture of products with possibly one ^{31}P NMR peak corresponding to what we would expect for the cyclometalated phosphine ligand on platinum (though in very low intensity). After getting the same results with

K_2CO_3, we decided to abandon this method, as purifying would be difficult because the complex is likely not stable to silica.

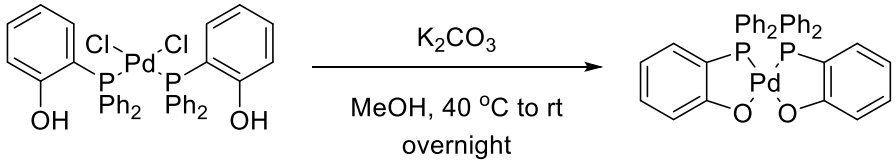

Figure 4.11. Cyclometalating a phosphine phenoxide on palladium

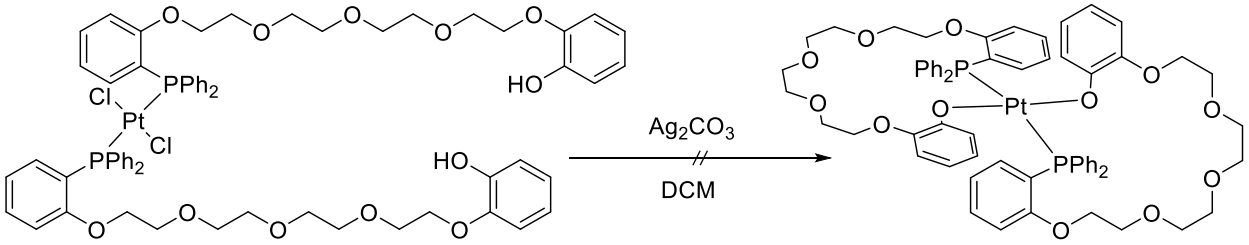

Figure 4.12. Cyclometalation attempt of *trans*-Cl_2Pt(phosphine ligand)$_2$ with Ag_2CO_3

Another method tried was heating the $PtMe_2$(phosphine ligand)$_2$ with a salt. $NaBPh_4$ or $LiPF_6$ were attempted with the rational that constraining the crown would lower the entropic cost of cyclometalating. However, after heating in NMR tubes with several solvents (C_6D_6, DMSO, and toluene), the desired product was not formed and the platinum complex decomposed.

Another group reported the method of putting the ligand in its sodium salt deprotonated form first and then reacting the ligand with a metal (Figure 4.13).[11] The first step was reacting the phosphine ligand with NaH (Figure 4.14). This seemed to work well with crude NMR having broader peaks and the phosphorous NMR shifting slightly (^{31}P NMR = -15.2 for deprotonated form vs. -15.5 for protonated form.)

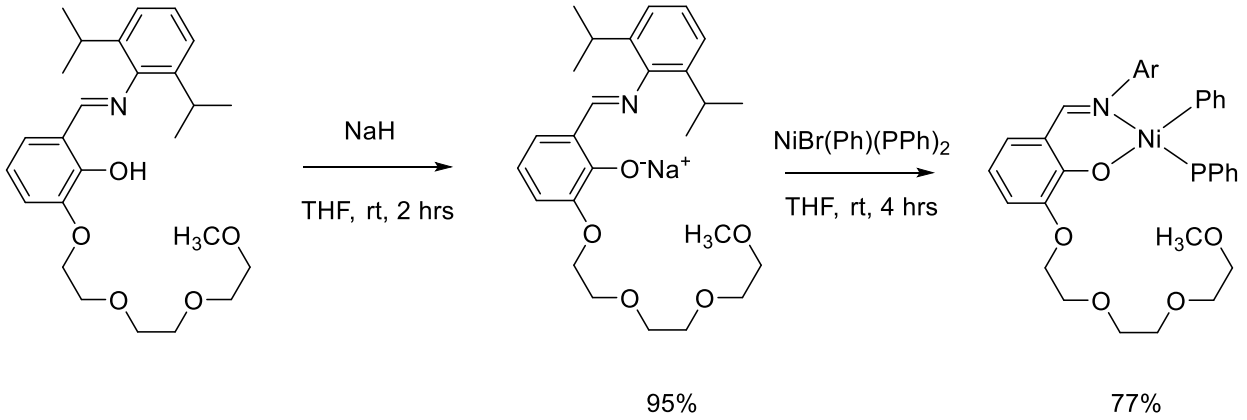

Figure 4.13. Do and coworkers cyclometallation through a salt molecule

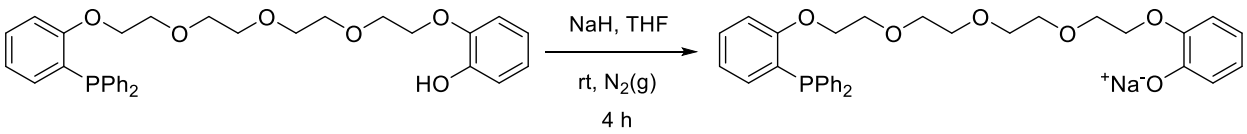

Figure 4.14. Formation of sodium salt form of phosphine ligand.

The next step is to react the sodium salt version of the phosphine ligand with a platinum chloride with two good leaving groups. This reaction is currently in progress and has promising results as monitored by NMR and is the next step in future work for this project.

Notes to Chapter 4

[1] Full procedures and characterization are in Chapter 5

[2] Pregosin, P. S.; Sze, S. N. *Helv. Chim. Acta* **1978**, *61*, 1848–1855.

[3] Grice, K. A.; Kositarut, J. A.; Lawando, A. E.; Sommer, R. D. *J. Organomet. Chem.* **2015**, *799-800*, 201–207.

[4] Haar, C. M.; Nolan, S. P.; Marshall, W. J.; Moloy, K. G.; Prock, A.; Giering, W. P. *Organometallics* **1999**, *18*, 474–479.

[5] Burrows, A. D.; Mahon, M. F.; Palmer, M. T. *J. Chem. Soc., Dalton Trans.* **2000**, *20*, 3615–3619.

[6] Massoni, M.; Clavijo, J. C. T.; Colina-Vegas, L.; Villarreal, W.; Dias, J. S.; Silva, G. A. D.; Ionta, M.; Soares, M.; Ellena, J.; Dorigueto, A. C.; Barbosa, M. I.; Batista, A. A. *Polyhedron* **2017**, *129*, 214–221.

[7] Dmitriev, V. I.; Timokhin, B. V.; Kalabina, A. V.; Samorodov, V. V. *Russ. J. Gen. Chem.* **1978**, *9*, 52-55

[8] Andrews, M. A.; Voss, E. J.; Gould, G. L.; Klooster, W. T.; Koetzle, T. F. *J. Am. Chem. Soc.* **1994**, *116*, 5730–5740.

[9] Andrews, M. A.; Gould, G. L.; Klooster, W. T.; Koenig, K. S.; Voss, E. J. *Inorg. Chem.* **1996**, *35*, 5478–5483.

[10] Heinicke, J.; Köhler, M.; Peulecke, N.; Keim, W.; Jones, P. G. *Z. Anorg. Allg. Chem.* **2004**, *630*, 1181–1190.

[11] Cai, Z.; Xiao, D.; Do, L. H. *J. Am. Chem. Soc.* **2015**, *137*, 15501–15510.

Chapter 5:

General Considerations

Reagents were used as received unless otherwise noted. Reactions under nitrogen were set up in a glovebox and sealed with a Teflon adapter. Reactions under argon were done using standard Schlenk line techniques. Column chromatography was performed with 230-400 mesh silica gel. When anhydrous reagents were needed, the reagent was left over 3Å sieves overnight. ^{31}P NMR was reference with external 75% H_3PO_4 in D_2O.

Synthesis

2-(2-(2-(2-hydroxyethoxy)ethoxy)ethoxy)ethyl 4-methylbenzenesulfonate

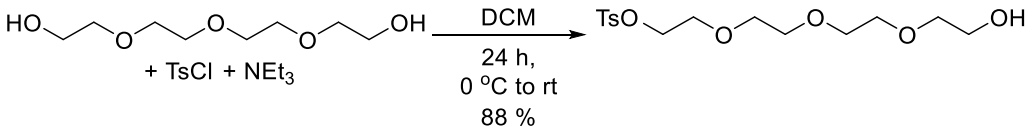

To a solution of tetraethylene glycol (42.1 g, 217 mmol) with triethylamine (5.1 g, 50 mmol) in dichloromethane (75 mL) at 0 °C was added tosyl chloride (6.19 g, 32.3 mmol) in approximately 100 mg portions over 1.5 h. The reaction mixture was warmed to room temperature (25 °C) and stirred for 24 h. The organic layer was washed with 3 × 50 mL of H_2O followed by 3 × 50 mL of a 7.5 g of citric acid in 150 mL H_2O solution. The organic layer was then dried over Na_2SO_4 and the volatiles were then removed in vacuo to yield (9.2 g, 81%) as a slightly yellow oil. ^1H NMR (300 MHz, $CDCl_3$) δ 7.76 (d, *J* = 8.4 Hz, 2H), 7.31 (d, *J* = 7.8 Hz, 2H), 4.18 – 4.08 (m, 2H), 3.73 – 3.48 (m, 14H), 2.63 (s, 1H), 2.41 (s, 3H). ^{13}C NMR (75 MHz, $CDCl_3$) δ 144.87, 132.97, 129.87, 127.98, 72.50, 70.73, 70.65, 70.47, 70.33, 69.31, 68.70, 61.70, 21.65.

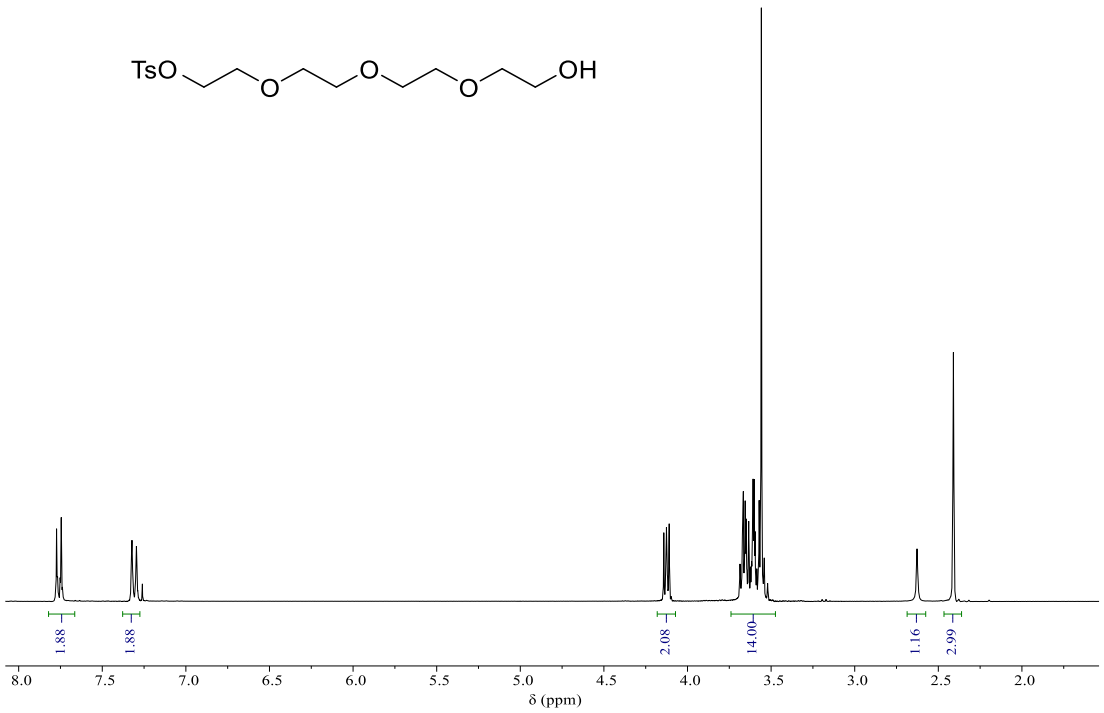
TsO
O
O
O
OH
1.88
1.88
2.08
14.00
1.16
2.99
8.0
7.5
7.0
6.5
6.0
5.5
5.0
4.5
4.0
3.5
3.0
2.5
2.0
δ (ppm)

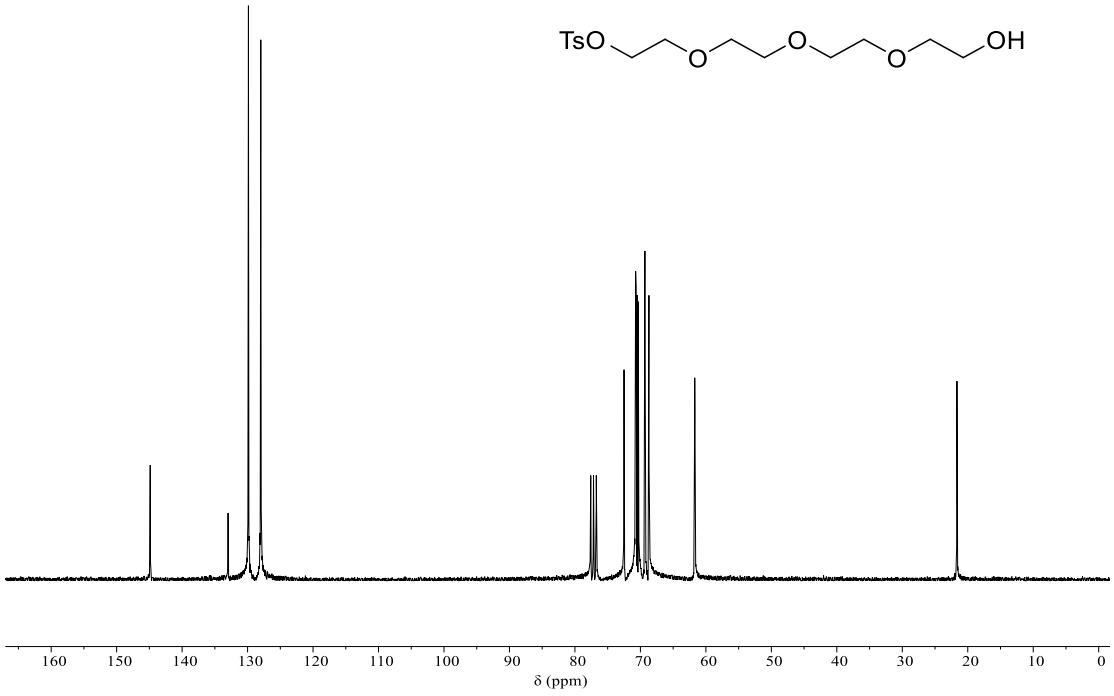
TsO
O
O
O
OH
160
150
140
130
120
110
100
90
80
70
60
50
40
30
20
10
0
δ (ppm)

2-(2-(2-(2-(2-iodophenoxy)ethoxy)ethoxy)ethoxy)ethan-1-ol

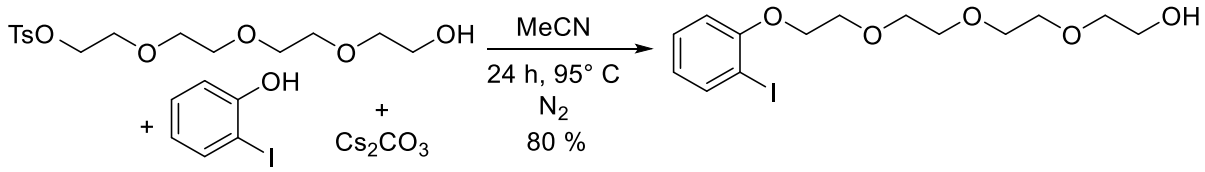

This synthesis is based on a literature procedure.[1] A 100 mL sealed reaction vessel was charged with cesium carbonate (4.14 g, 12.7 mmol), 2-iodophenol (2.00 g, 9.08 mmol), and mono tosyl tetraethylene glycol (3.16 g, 9.08 mmol) in MeCN (50 mL) under N_2 (g). The reaction vessel was then heated to 105 ºC and stirred for 24 hours. The reaction mixture was then cooled to room temperature and the solvent was removed in vacuo. The remaining material was extracted with DCM (3 × 75 mL). The extracts were filtered, and then washed with brine (3 × 200mL). The volatiles were then removed in vacuo to yield a slightly yellow oil (3.16 g, 88%) ^{1}H NMR (500 MHz, $CDCl_3$) δ 7.76 (1H, dd, *J* = 7.77 and 1.63 Hz), 7.27 (1H, ddd, *J* = 8.43, 7.47, and 1.74 Hz), 6.83 (1H, dd, *J* = 8.26 and 1.37 Hz), 6.70 (1H, td, *J* = 7.60 and 1.39 Hz), 4.20-4.14 (2H, m), 3.97-3.89 (2H, m), 3.86-3.78 (2H, m), 3.78 – 3.57 (m, 10H), 2.51 (1H, br) ^{13}C NMR (75 MHz, $CDCl_3$) δ 157.58, 139.58, 129.57, 122.87, 112.56, 86.76, 72.60, 71.32, 70.81, 70.75, 70.46, 69.63, 69.23, 61.85.

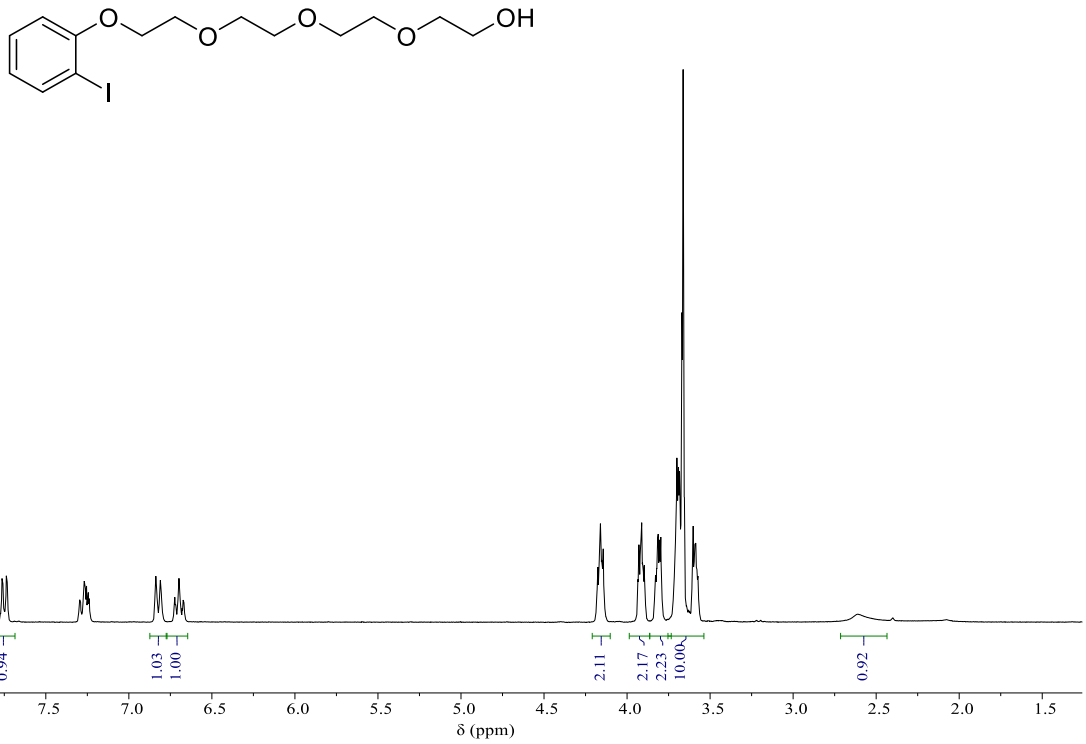

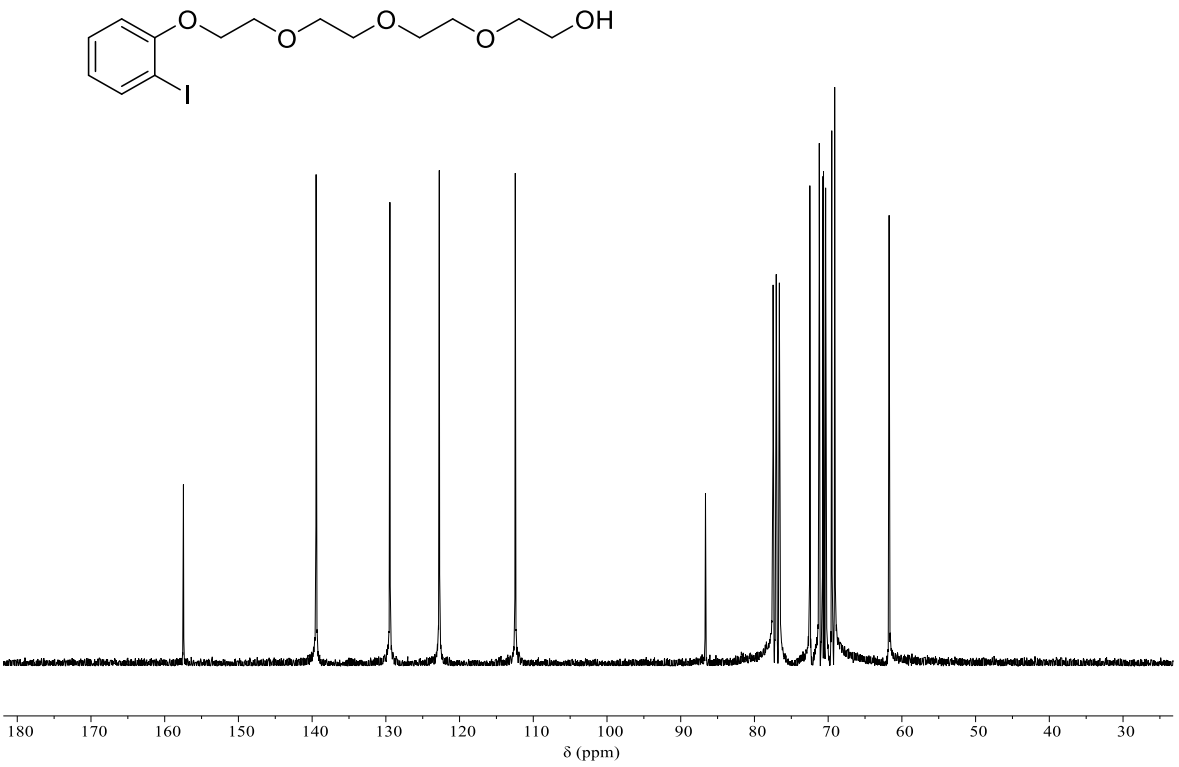

2-(2-(2-(2-(2-iodophenoxy)ethoxy)ethoxy)ethoxy)ethyl 4-methylbenzenesulfonate

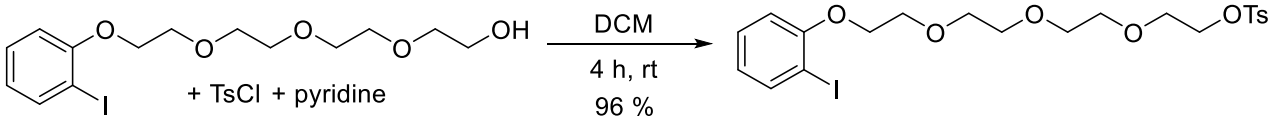

This synthesis is based on a literature procedure.[2] A suspension of 2-(2-(2-(2-(2-iodophenoxy)ethoxy)ethoxy)ethoxy)ethan-1-ol (1.3 g, 3.3 mmol) and tosyl chloride (1.9 g, 9.8 mmol) were dissolved in pyridine (22.5 mL) and stirred at room temperature (23 ºC) for 4 hours. 1M HCl (175 mL) was then added and the reaction was stirred for another hour. The reaction mixture was then diluted with DCM (200 mL). The DCM extracts were then washed with 1M HCl (4 ×150 mL) and brine (2 ×150 mL). The organic layer was then dried over $MgSO_4$ and solvent removed in vacuo to yield the slightly yellow oil 2-(2-(2-(2-(2-iodophenoxy)ethoxy)ethoxy)ethoxy)ethyl 4-methylbenzenesulfonate (1.4 g, 78% yield) ^{1}H NMR (500 MHz, $CDCl_3$) δ 7.83 – 7.71 (m, 3H), 7.33 (dd, *J* = 8.5, 0.8 Hz, 2H), 7.31 – 7.26 (m, 1H), 6.83 (dd, *J* = 8.2, 1.4 Hz, 1H), 6.71 (td, *J* = 7.6, 1.4 Hz, 1H), 4.16 (dt, *J* = 6.9, 4.8 Hz, 4H), 3.96 – 3.89 (m, 2H), 3.84 – 3.76 (m, 2H), 3.71 – 3.63 (m, 4H), 3.62 – 3.56 (m, 4H) 2.44 (s, 3H) ^{13}C NMR (75 MHz, $CDCl_3$) δ 157.54, 144.85, 139.52, 133.07, 129.89, 129.55, 128.04, 122.82, 112.53, 86.72, 71.26, 70.84, 70.82, 70.63, 69.59, 69.34, 69.19, 68.74, 21.72.

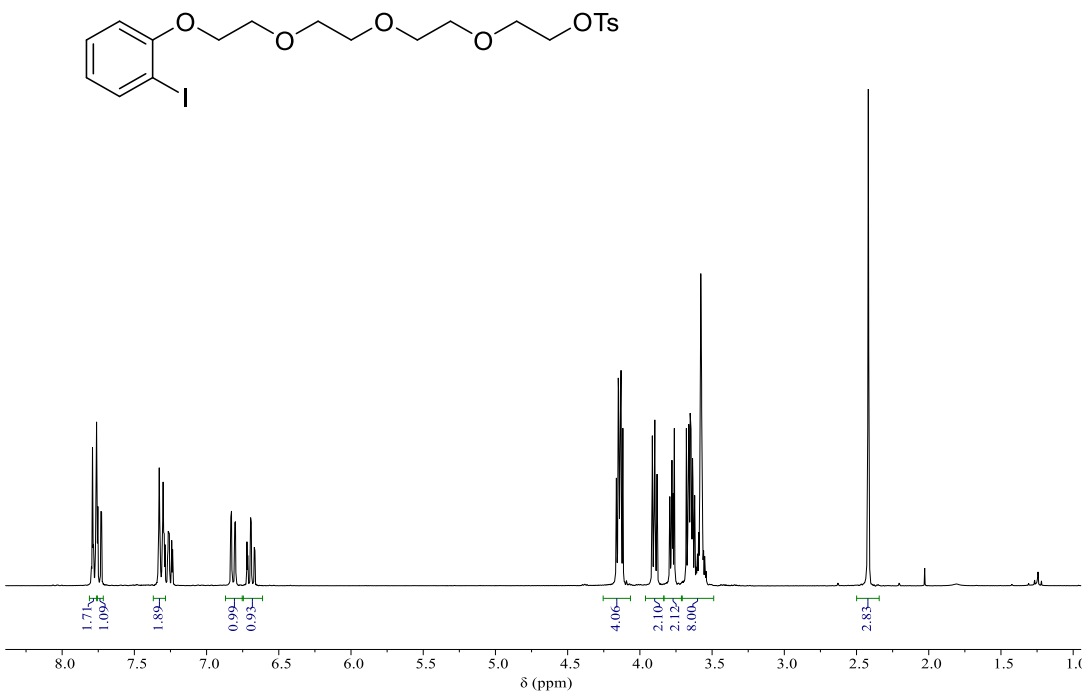
O
O
O
O
OTs
I
1.71
1.09
1.89
0.99
0.93
4.06
2.10
2.12
8.00
2.83
8.0
7.5
7.0
6.5
6.0
5.5
5.0
4.5
4.0
3.5
3.0
2.5
2.0
1.5
δ (ppm)

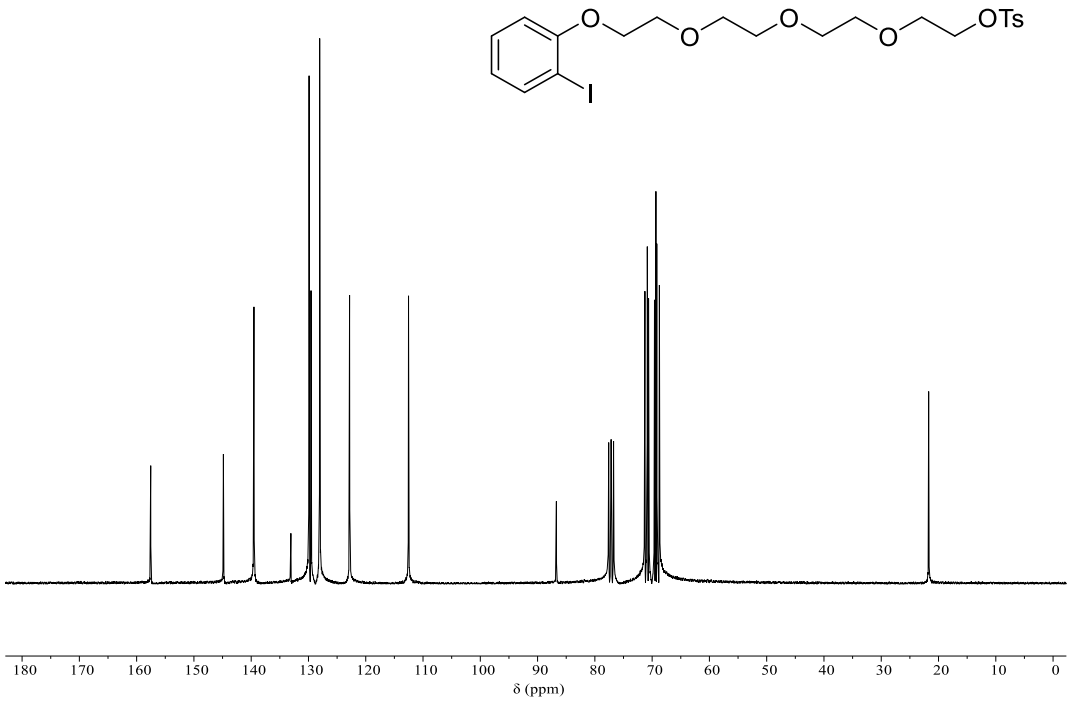
O
O
O
O
OTs
I
180
170
160
150
140
130
120
110
100
90
80
70
60
50
40
30
20
10
0
δ (ppm)

2-(2-(2-(2-(2-(2-iodophenoxy)ethoxy)ethoxy)ethoxy)ethoxy)phenol

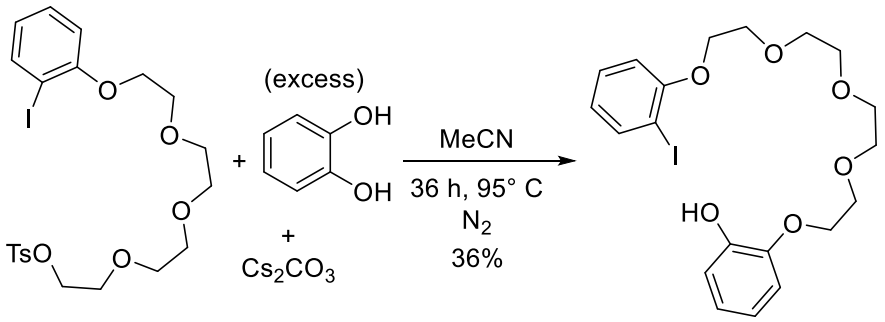

A 100 mL Teflon sealed reaction vessel was charged with 2-(2-(2-(2-(2-iodophenoxy)ethoxy)ethoxy)ethoxy)ethyl 4-methylbenzenesulfonate (2.5 g, 4.5 mmol), catechol (3.4 g, 31 mmol), and cesium carbonate (5.0 g, 15 mmol) and dried acetonitrile (60 mL). The mixture was stirred under nitrogen gas at 95 ºC for 36 hours during which time a solid formed. The reaction mixture was cooled to room temperature and the solvent was removed in vacuo. The reaction mixture was then extracted with DCM (4 × 50 mL) and filtered. The mixture was purified by column chromatography on silica, 6:4 hexanes/ethyl acetate to 3:7 hexanes/ethyl acetate to yield 2-(2-(2-(2-(2-(2-iodophenoxy)ethoxy)ethoxy)ethoxy)ethoxy)phenol (0.798 g, 36%) as a yellowish oil. ^{1}H NMR (500 MHz, $CDCl_3$) δ 7.76 (dd, *J* = 7.8, 1.6 Hz, 1H), 7.30 – 7.25 (m, 1H), 6.96 – 6.88 (m, 3H), 6.85 – 6.77 (m, 2H), 6.74 – 6.67 (m, 2H), 4.21 – 4.13 (m, 4H), 3.93 (dd, *J* = 5.5, 4.4 Hz, 2H), 3.86 – 3.79 (m, 4H), 3.76 – 3.66 (m, 6H). ^{13}C NMR (126 MHz, $CDCl_3$) δ 157.56, 147.59, 146.15, 139.53, 129.58, 122.94, 122.84, 119.87, 115.86, 115.04, 112.61, 86.73, 77.41, 77.16, 76.91, 71.32, 70.77, 70.72, 70.54, 69.70, 69.64, 69.59, 69.15.

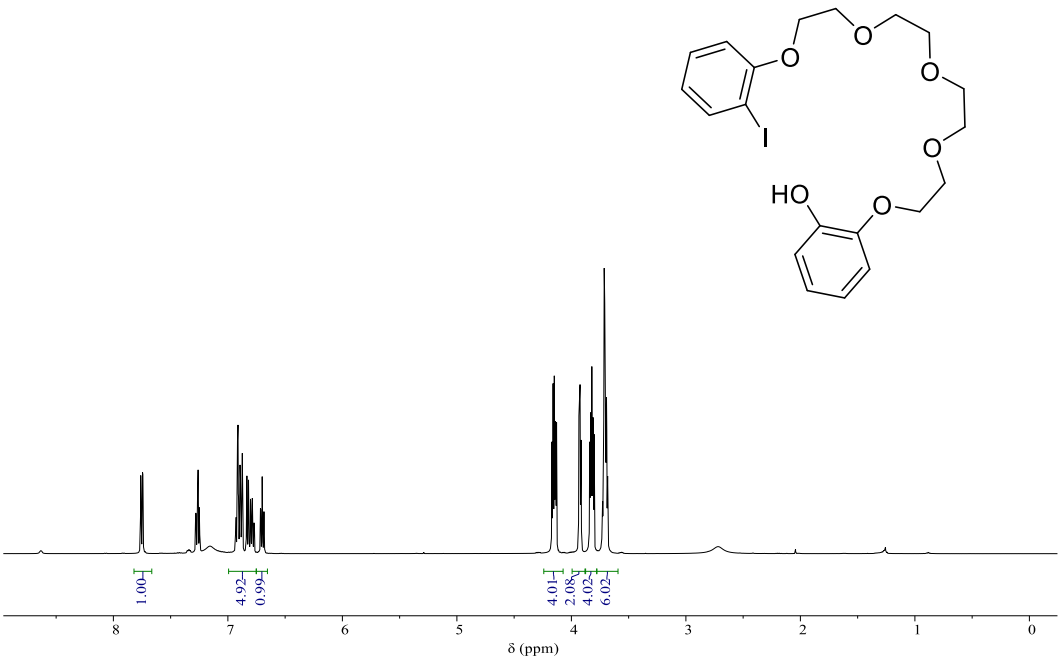

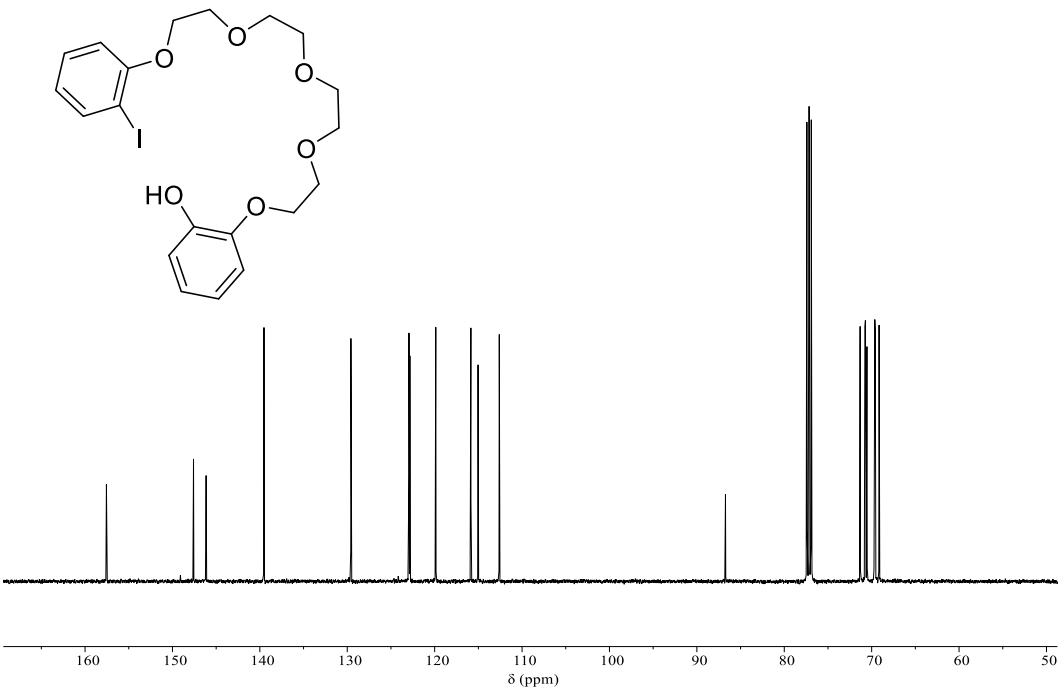

(2-(2-(2-(2-(2-(2-iodophenoxy)ethoxy)ethoxy)ethoxy)ethoxy)phenyl)diphenylphosphane

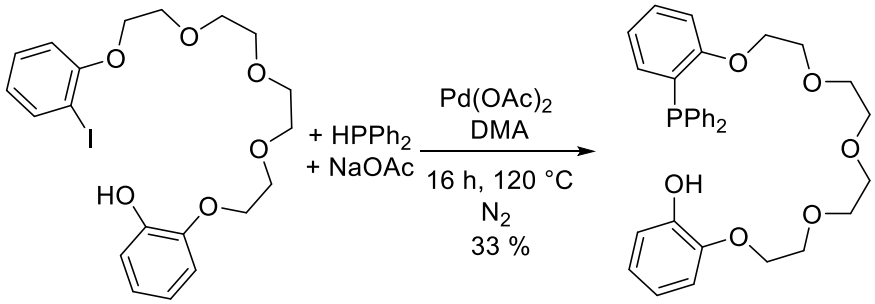

A 100 mL Teflon sealed reaction vessel was charged with 2-(2-(2-(2-(2-(2-iodophenoxy)ethoxy)ethoxy)ethoxy)ethoxy)phenol (0.5 g, 1.0 mmol), sodium acetate (0.092 g, 1.1 mmol), $Pd(OAc)_2$ (2.3 mg, 0.010 mmol), and diphenylphosphane (0.18 mL, 1.02 mmol) in DMA (40 mL) under N_2 (g) and heated to 120 ºC for 16 hours. In air the reaction mixture was then filtered through celite and DMA was removed by vacuum filtration. The mixture was purified by column chromatography on silica by DCM to 3:7 ethyl acetate to yield the yellow oil (2-(2-(2-(2-(2-(2-iodophenoxy)ethoxy)ethoxy)ethoxy)ethoxy)phenyl)diphenylphosphane (180 mg, 33%). ^{1}H NMR (500 MHz, $CDCl_3$) δ 7.35 – 7.26 (m, 11H), 6.94 – 6.74 (m, 7H), 6.65 (ddd, *J* = 7.5, 4.8, 1.7 Hz, 1H), 4.18 – 4.09 (m, 2H), 4.03 (t, *J* = 5.0 Hz, 2H), 3.84 – 3.74 (m, 2H), 3.73 – 3.66 (m, 2H), 3.66 – 3.59 (m, 2H), 3.54 (dd, *J* = 5.4, 4.7 Hz, 2H), 3.46 (s, 4H). ^{13}C NMR (126 MHz,$CDCl_3$) δ 160.26 (d, *J* = 14.8 Hz), 147.61, 146.16, 136.84 (d, *J* = 10.4 Hz), 134.05 (d, *J* = 20.3 Hz), 133.52 (d, *J* = 2.0 Hz), 130.33, 128.70, 128.46 (d, *J* = 7.0 Hz), 126.10 (d, *J* = 12.6 Hz),

122.94, 121.32, 119.87, 115.85, 115.09, 111.39 (d, J = 1.6 Hz), 70.89, 70.67, 70.62, 70.42, 69.73, 69.61, 69.34, 68.50. ^{31}P NMR (202 MHz, $CDCl_3$) δ -15.5

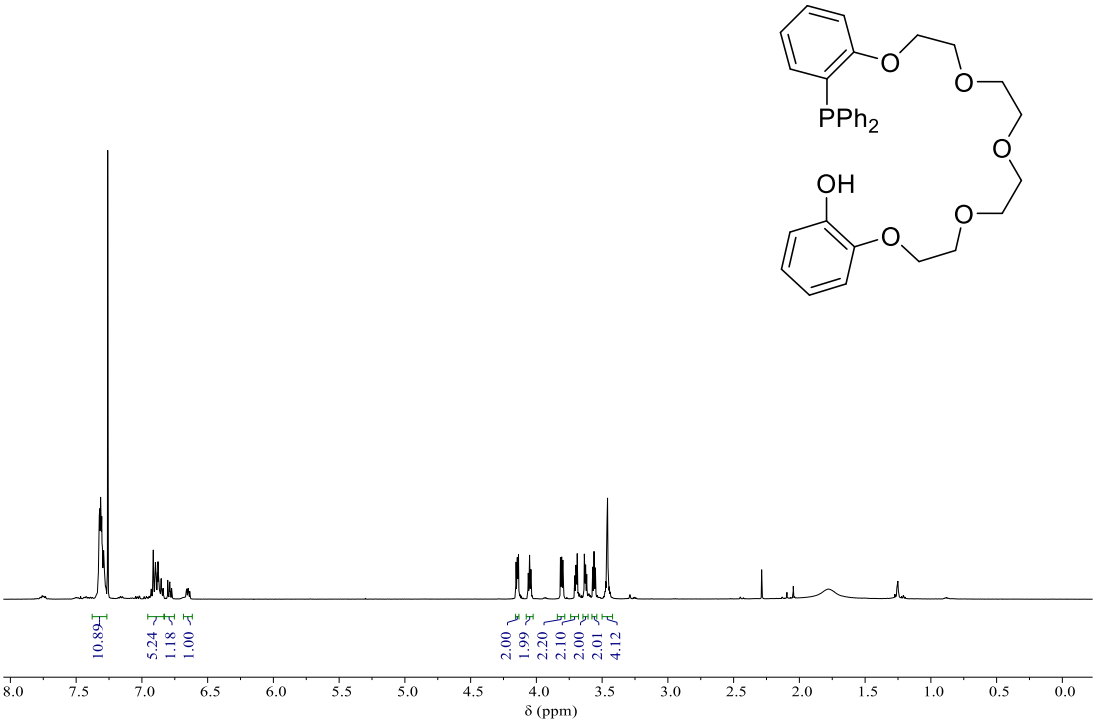

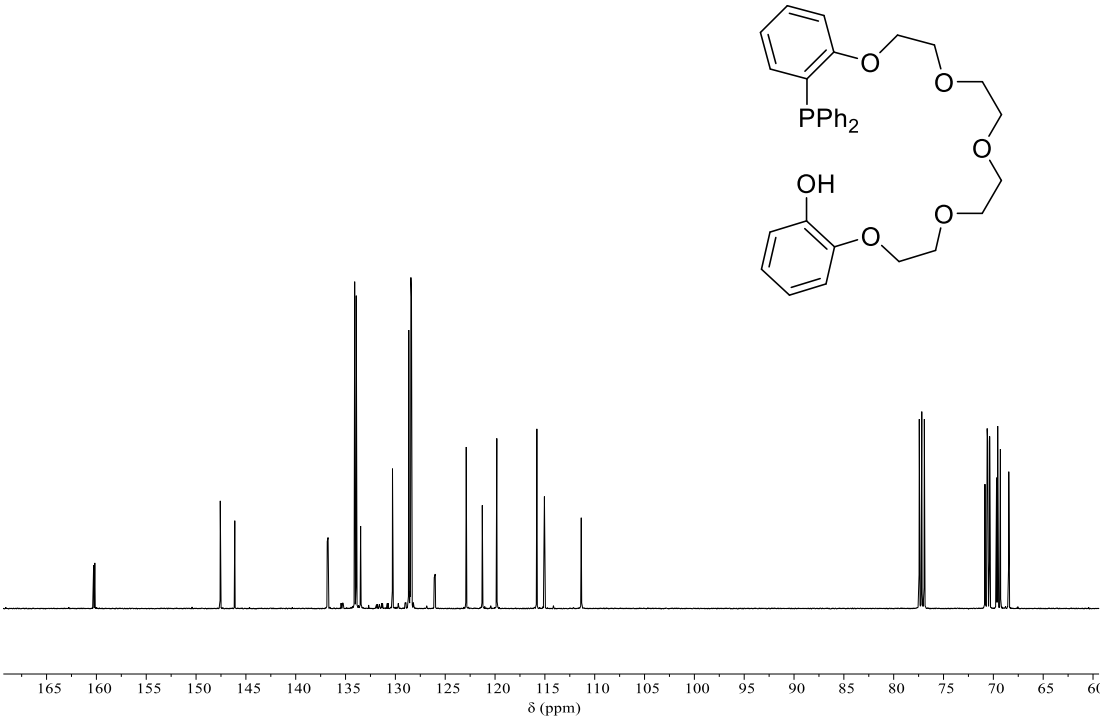

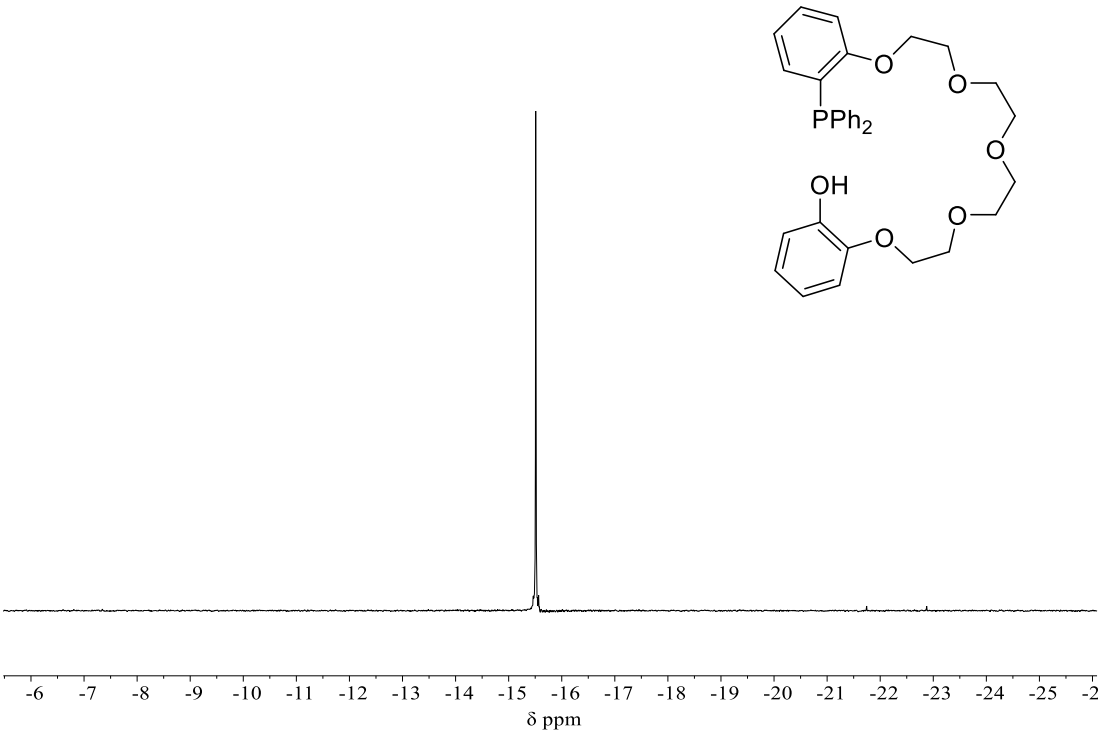

$PtCl_2$(bis-phosphine ligand)

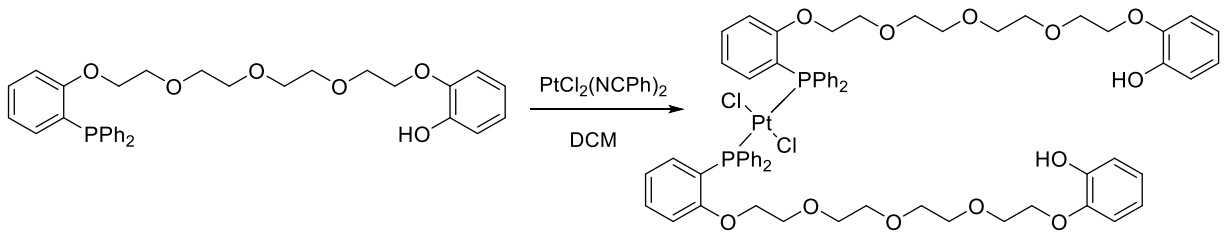

A solution of $PtCl_2(NCPh)_2$ (28 mg, 0.073 mmol) and phosphine ligand (80 mg, 0.15 mmol) in DCM (15 mL) was stirred at room temperature for 24 hours. The solvent was then removed and the reaction mixture was washed with water (3 × 5 mL) to yield a yellow solid (76 mg, 81%). The *trans* isomer slowly converted to a mixture of *cis* and *trans* over a week. *Trans* isomer could be purified by column chromatography on silica by 1:1 DCM/ethyl acetate.

NMR data of the *trans* isomer

^{1}H NMR (500 MHz, $CDCl_3$) δ 7.88-7.76 (m, 4H), 7.42-7.29 (m, 7H), 7.13-7.05 (m, 1H), 6.97-6.84 (m, 5H), 6.83-6.76 (m, 1H), 4.16 – 4.12 (m, 2H), 4.06 (t, *J* = 5.2 Hz, 2H), 3.80 – 3.76 (m, 2H), 3.70 – 3.64 (m, 2H), 3.60 – 3.57 (m, 2H), 3.55 (t, *J* = 5.2 Hz, 2H), 3.35 (m, *J* = 6.0, 3.1 Hz, 2H), 3.31 – 3.28 (m, 2H). ^{13}C NMR (126 MHz, Benzene-d_6) δ 160.74 (d, *J* = 4.1 Hz), 148.88, 146.94, 135.99 (t, *J* = 5.7 Hz), 135.29, 132.74, 130.57, 130.34, 130.17, 130.11, 123.37, 120.71 (t, *J* = 8.4, 4.1 Hz), 119.80, 118.32 (t, *J* = 29.5 Hz), 116.64, 115.51, 112.18, 70.84, 70.78, 70.74, 70.54, 69.68, 69.56, 69.52, 68.71. ^{13}P NMR (202 MHz,$CDCl_3$) δ 13.88 (trans $J_{P\text{-}Pt}$ = 2698 Hz)

For *cis* isomer

^{31}P NMR (202 MHz, $CDCl_3$) δ 8.46 (Cis $J_{P\text{-}Pt}$ = 3801 Hz)

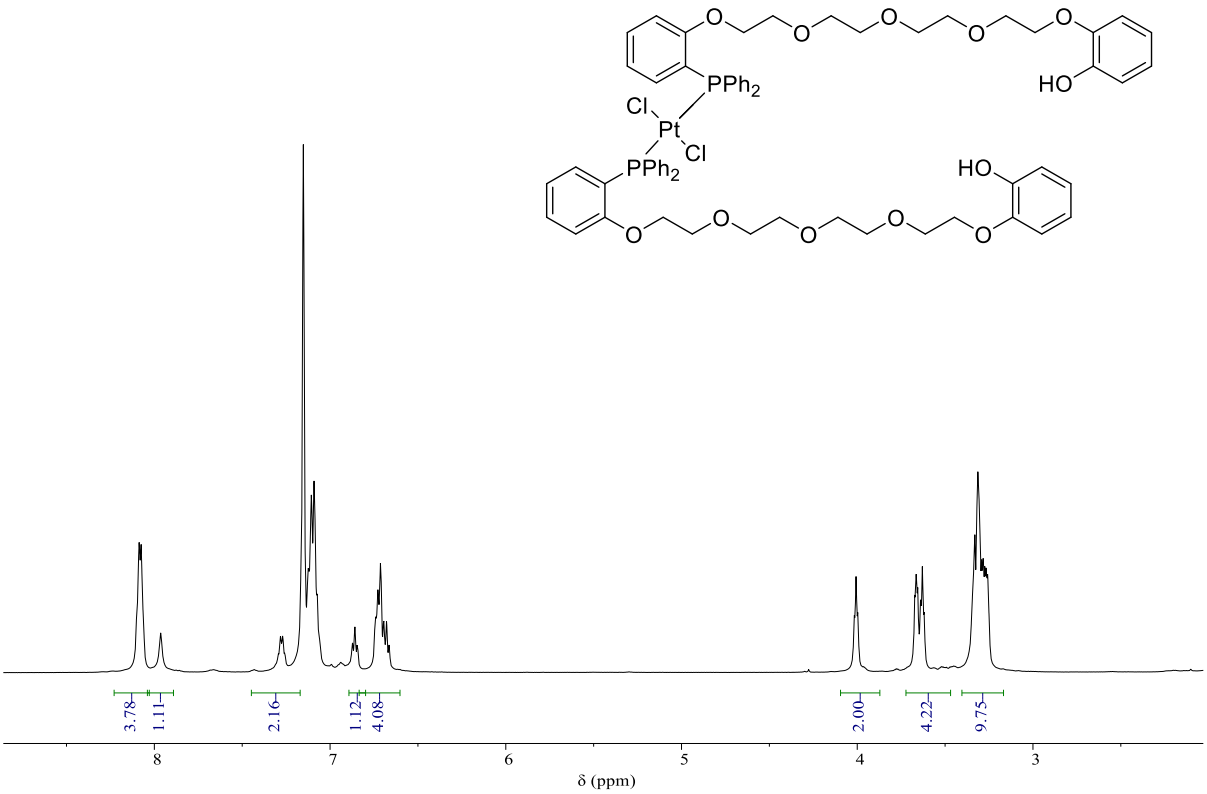

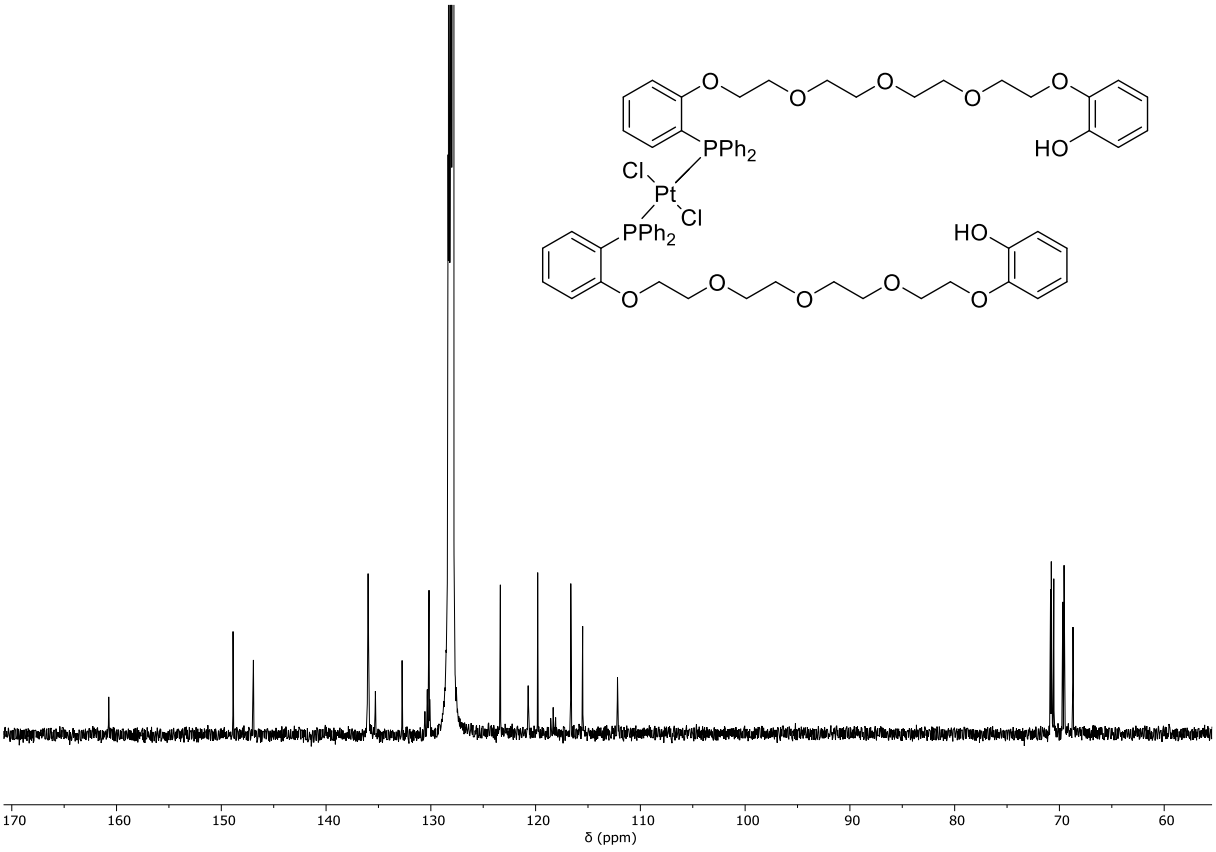
O
O
O
O
O
HO
PPh2
Cl
Pt
Cl
PPh2
HO
O
O
O
O
O
170
160
150
140
130
120
110
100
90
80
70
60
δ (ppm)

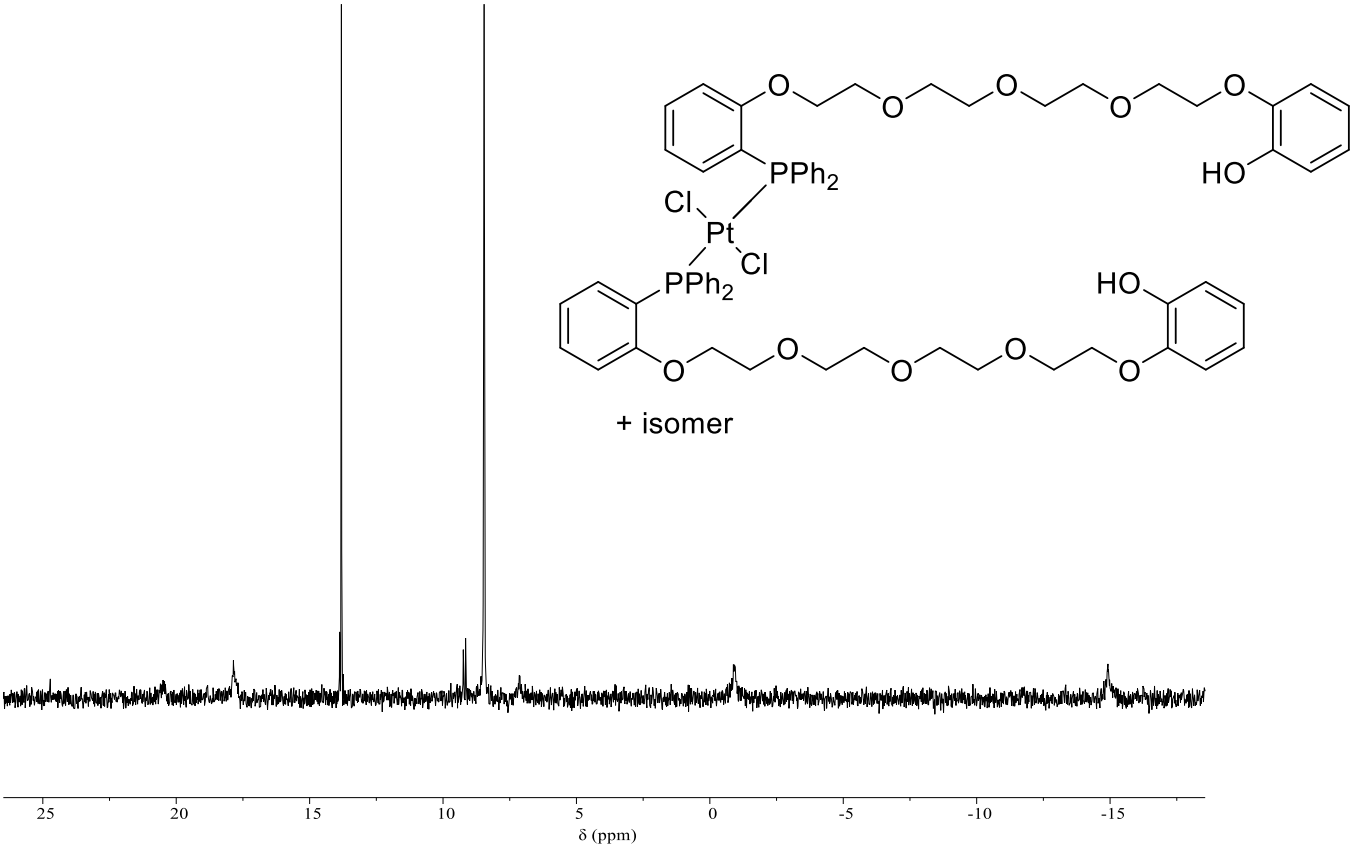
O
O
O
O
O
HO
PPh2
Cl
Pt
Cl
PPh2
HO
O
O
O
O
O
+ isomer
25
20
15
10
5
0
-5
-10
-15
δ (ppm)

Dichlorobis(diethyl sulfide)platinum(II)

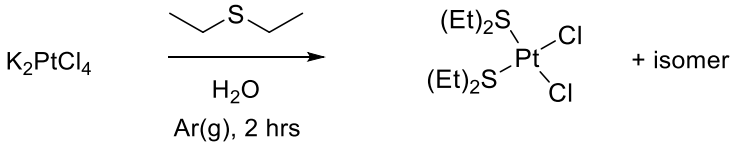

This synthesis is based on a literature procedure.[3] To a round bottom flask with K_2PtCl_4 (630 mg, 1.52 mmol) and water (20 mL) under argon was added diethyl sulfide (.475 mL, 4.41 mmol) and stirred at reflux for 2 hours. The reaction mixture was then extracted with DCM (2 × 70 mL) and dried over $MgSO_4$. The solvent was then removed in vacuo to yield .6 g of the bright yellow solid dichlorobis(diethyl sulfide)platinum(II). (91%) ^{1}H NMR (500 MHz, $CDCl_3$) δ 3.22 (dq, *J* = 12.0, 7.5 Hz, 2H), 2.68 (dq, *J* = 12.1, 7.3 Hz, 2H), 1.42 (t, *J* = 7.4 Hz, 1H), 1.38 (t, *J* = 7.4 Hz, 5H).

$[(SEt_2)PtMe_2]_2$

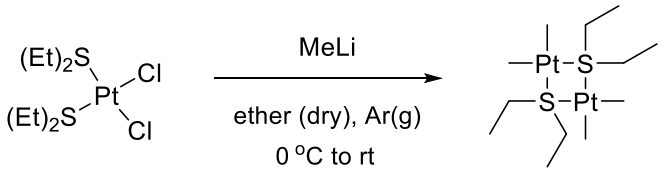

To a solution of dichlorobis(diethyl sulfide)platinum(II) (200 mg, .448 mmol) and dry ether (25 mL) in an ice bath under argon gas was added methyl lithium (1.55 mL, 1.6 M) in ether. The reaction mixture was stirred overnight and slowly brought to room temperature and water (1.5 mL) was added slowly. Then water (40 mL) was added to the reaction mixture and was extracted with DCM (2 × 60 mL) and dried over Na_2SO_4. The solvent was then removed in vacuo and product was recrystallized three times with acetone to yield the brown solid $[(Set_2)PtMe_2]_2$. (67 mg, 24%). ^{1}H NMR (500 MHz, $CDCl_3$) δ 3.07 (q, *J* = 7.4 Hz, 2H), 1.64 (t, *J* = 7.4 Hz, 3H), 0.52 (d, $J_{Pt\text{-}H}$ = 85.0 Hz, 3H).

$Pt(P)_2Me_2$

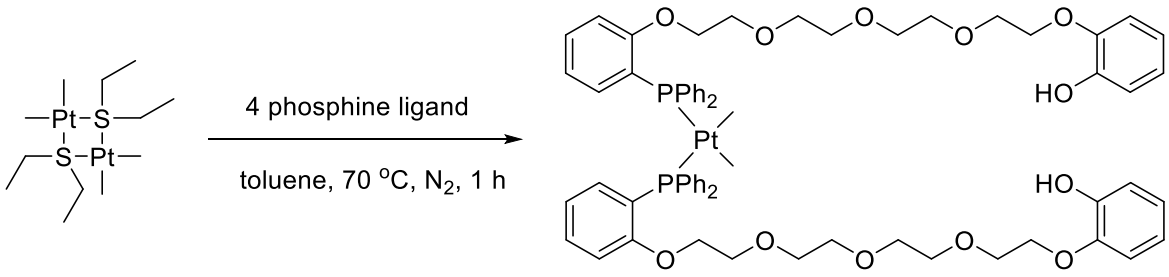

To a sealed reaction vessel was added $[PtMe_2SEt_2]_2$ (3.32 mg, 0.0053 mmol) and the phosphine ligand (11.5 mg, 0.0210 mmol) in toluene was stirred at 70 °C under N_2(g) for 45 min. The solvent was then removed in vacuo to yield of a brownish/black paste (10 mg, 77%). ^{1}H NMR (500 MHz, C_6D_6) δ 7.76 – 7.64 (m, 4H), 7.59 (t, *J* = 9.6 Hz, 1H), 7.11 – 7.17 (m, 1H), 7.07 – 6.90 (m, 7H), 6.90 – 6.79 (m, 1H), 6.80 – 6.61 (m, 3H), 6.42 (d, *J* = 6.6 Hz, 1H), 3.74 – 3.65 (m, 2H), 3.62 (t, *J* = 5.8 Hz, 2H), 3.45 – 3.30 (m, 8H), 3.30 – 3.23 (m, 2H), 3.18 (t, *J* = 5.8 Hz, 2H),

1.11 (tt, $J_{Pt\text{-}H}$ = 36.76 Hz, $J_{H\text{-}H}$ = 6.0 Hz, 2H). ^{31}P NMR (202 MHz, C_6D_6) δ 24.72 (d, $J_{Pt\text{-}P}$ = 1940.0 Hz)

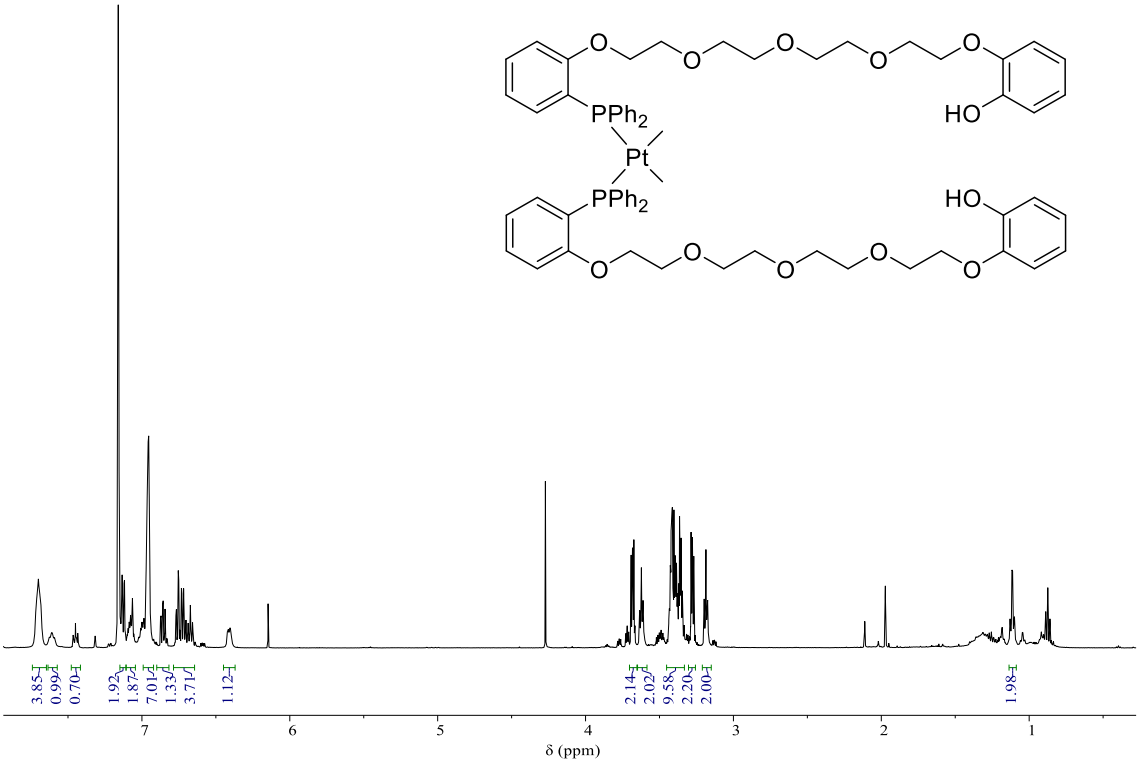

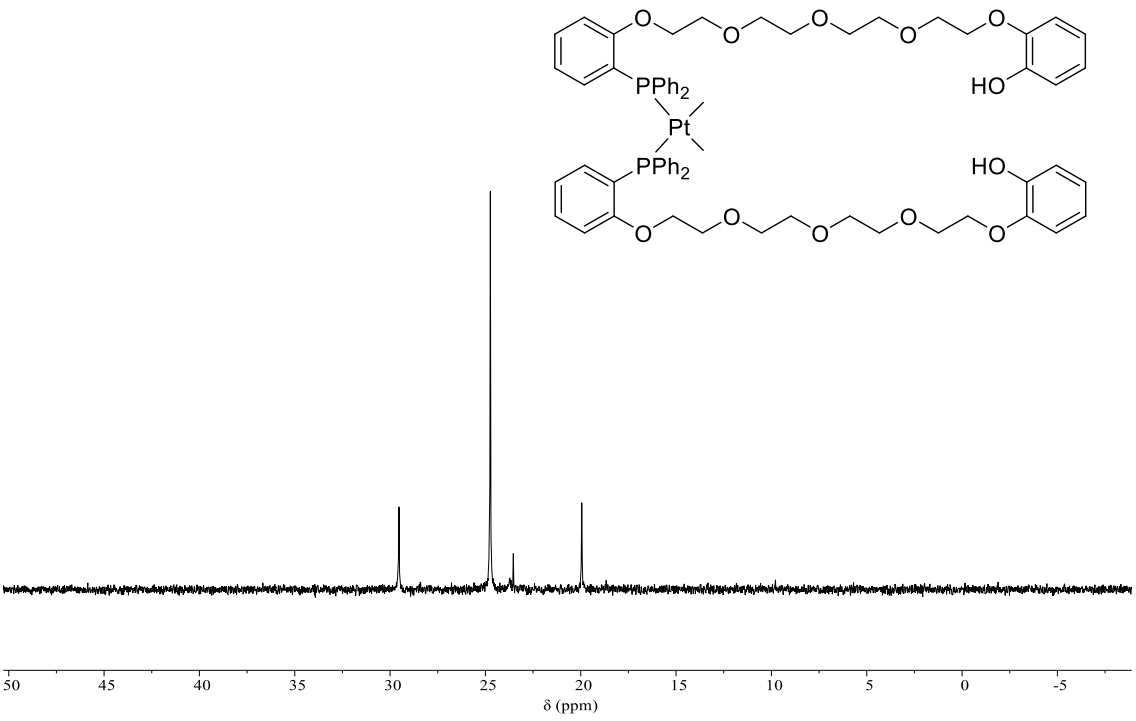

Sodium 2-(2-(2-(2-(2-(2-(diphenylphosphaneyl)phenoxy)ethoxy)ethoxy)ethoxy)ethoxy)phenolate.

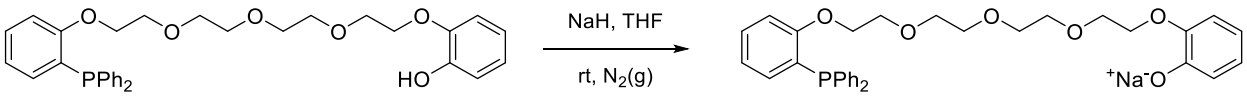

To a solution under N_2(g) was added phosphine ligand (12 mg, 0.0219 mmol) and NaH (1 mg, 0.043 mmol) in THF (3 mL) and stirred for 2 hrs and then left to sit overnight. The reaction was then filtered through celite and solvent removed in vacuo. ^{1}H NMR (500 MHz, C_6D_6) δ 7.49-7.35 (m, 4H), 7.20-6.95 (m, 9H), 6.91 (ddd, *J* = 7.6, 4.6, 1.7 Hz, 1H), 6.82-6.72 (s br, 1H), 6.71 (t, *J* = 7.4 Hz, 2H), 6.57 (td, *J* = 7.5, 1.7 Hz, 1H), 3.87 (s, 2H), 3.69 – 3.61 (m, 2H), 3.51 – 3.40 (m, 2H), 3.31 – 3.06 (m, 11H). ^{31}P NMR (202 MHz, $CDCl_3$) δ -15.2

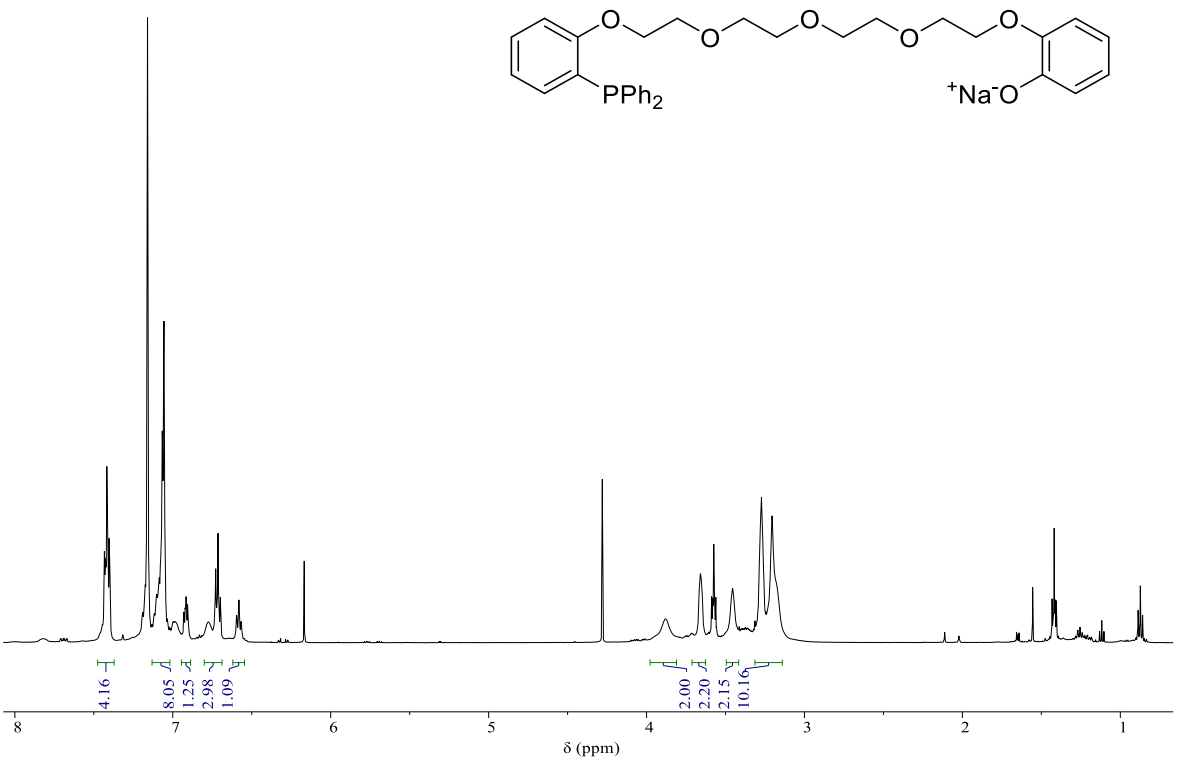

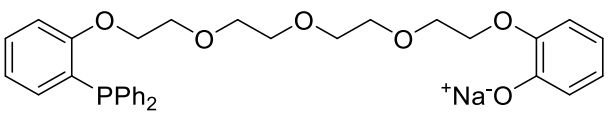

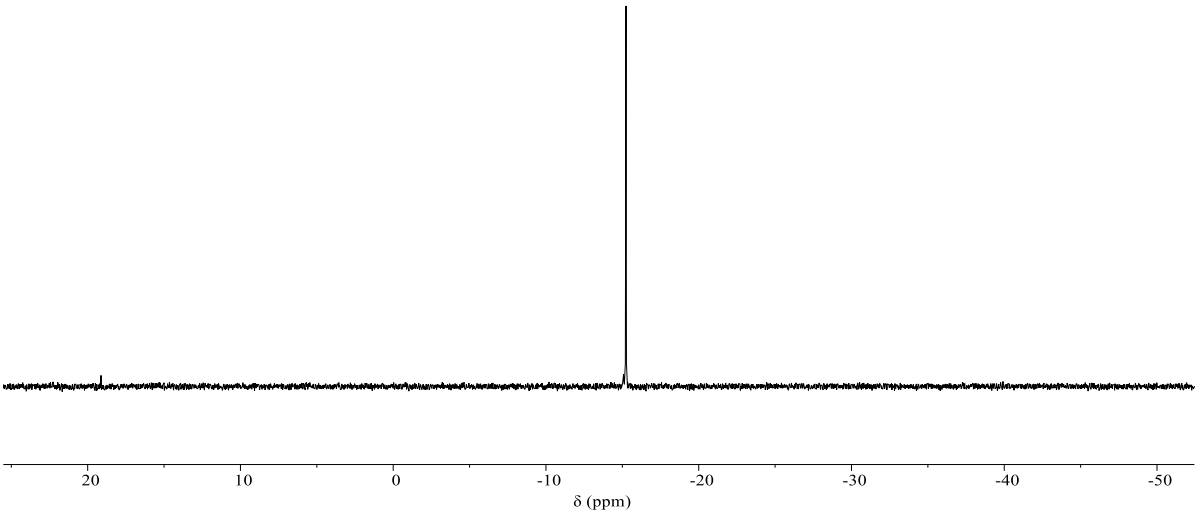

Notes to Chapter 5

[1] Song, F.-T.; Ouyang, G.-H.; Li, Y.; He, Y.-M.; Fan, Q.-H. *Eur. J. Org. Chem*. **2014**, *30*, 6713–6719.

[2] Elhalem, E.; Bailey, B. N.; Docampo, R.; Ujváry, I.; Szajnman, S. H.; Rodriguez, J. B. *J. Med. Chem.* **2002**, *45*, 3984–3999.

[3] Juvenal, F.; Langlois, A.; Bonnot, A.; Fortin, D.; Harvey, P. D. *Inorg. Chem.* **2016**, *55*, 11096–11109.